Pharmacological Research 229 (2026) 108237

Contents lists available at ScienceDirect

Pharmacological Research

journal homepage: www.elsevier.com/locate/yphrs

FDA-approved RET protein-tyrosine kinase inhibitors in the management of RET-driven thyroid and lung cancer

Robert Roskoski Jr.

Blue Ridge Institute for Medical Research, 221 Haywood Knolls Drive, Hendersonville, NC 28791, United States

ARTICLE INFO

Keywords:
Follicular lung cancer
Medullary lung cancer
Multiple endocrine neoplasia
Papillary lung cancer
RET mutations and fusion proteins
Targeted cancer therapy

Chemical compounds studied in this article:
Cabozantinib (PubMED CID: 25102847)
I^{131} (PubMED CID: 10220516)
Imatinib (PubMED CID: 5291)
Lenvatinib (PubMED CID: 9823820)
Levothyroxine (PubMED CID: 5819)
Pralsetinib (PubMED CID: 129073603)
Selpercatinib (PubMED CID: 124436908)
Sorafenib (PubMED CID: 216239)
Sunitinib (PubMED CID: 5329102
Vandetanib (PubMed CID: 3081361)

ABSTRACT

RET is a transmembrane receptor protein-tyrosine kinase that is required for the (i) survival and maturation of the enteric nervous system, the autonomic nervous system, and sensory neurons, (ii) renal development, and (iii) spermatogenesis. RET activation by its glial-cell derived neurotrophic factor (GDNF) ligands differs from that of all other receptor protein-tyrosine kinases because of the requirement for additional GDNF family receptor-α co-receptors (GFRα1/2/3/4, GFRAL). Activating *RET*-point mutations occur in multiple endocrine neoplasia syndromes (MEN2A, MEN2B) and in isolated medullary thyroid cancer. RET-fusion proteins, commonly KIF5B-RET, occur in NSCLC. More than three dozen fusion partners of RET have been described in papillary thyroid cancer. Several multikinase blockers targeting RET have been approved by the FDA for the treatment of cancer: (i) vandetanib for medullary thyroid carcinoma and (ii) cabozantinib, lenvatinib, and sorafenib for differentiated thyroid cancer. Pralsetinib is a specific RET blocker that is FDA-approved for the treatment of medullary thyroid cancer, RET-fusion positive thyroid cancer and NSCLC. Selpercatinib is FDA-approved for the management of *RET*-mutant medullary thyroid cancer, RET-fusion-positive thyroid cancer, and other RET-fusion-positive solid tumors. The RET signaling pathway participates in the pathogenesis of cancer, particularly in thyroid and lung cancer. Currently, the number of new cases of thyroid cancer bearing *RET* mutations or RET-fusion proteins is about 13,000 per year and the number of cases of RET-driven NSCLC range from about 2000–4000 per year in the United States. Inactivating *RET* mutations result in Hirschsprung disease, a congenital disorder leading to aganglionosis of the gastrointestinal tract.

1. An overview of RET protein-tyrosine kinase

As they reported in 1985, Takahashi et al. transformed normal murine NIH 3T3 fibroblasts with sonicated human lymphoma DNA into cancer-like cells [1]. They found that the transforming DNA sequence consisted of 34 kilobases and contained a rearrangement of two normal but physiologically unlinked DNA segments. Because this transforming DNA was the product of gene rearrangement during transfection, they dubbed it "REarranged during Transfection," or RET. Ishizaka et al. found that the human *RET* gene resides on chromosome 10 (10q11.2) [2]. Durbee et al. later identified RET as the protein-tyrosine kinase receptor for GDNF (glial-cell derived neurotrophic factor) [3]. In addition to GDNF, this family includes artemin (ARTN), neurturin (NRTN), persephin (PSPN), and growth differentiation factor 15 (GDF15) [4]. The closest homologs of the RET receptor protein-tyrosine kinase are FGFR1/2/3/4 and VEGFR1/2/3 [5]. RET is required for the development of the nervous system, the thyroid gland, the lung, the testes, calcitonin producing C-cells of the thyroid, and the intestinal epithelium [4]. We will consider the role of RET in the pathogenesis of thyroid cancer, multiple endocrine neoplasias (MEN2A, MEN2B), and lung cancer.

The activation mechanism of RET by its ligands differs from that of

Abbreviations: ARTN, artemin; AS, activation segment; CD, cadherin-like domain; CL, catalytic loop; CS or C-spine, catalytic spine; CTT, carboxyterminal tail; EGFR, epidermal growth factor receptor; FDA, the United States Food and Drug Administration; FGFR, fibroblast growth factor receptor; FMTC, familial medullary lung cancer; GDF15, growth differentiation factor 15; GDNF, glial-cell derived neurotrophic factor; GFRα, GDNF family receptor-α; GFRAL, GDNF family receptor α-like; GK, gatekeeper; GPI, glycosylphosphatidylinositol; GRL, Gly-rich loop; JM, juxtamembrane segment; KID, kinase insert domain; MEN, multiple endocrine neoplasia; MTC, medullary thyroid cancer; NRTN, neurturin; NSCLC, non-small cell lung cancer; PDGFR, platelet-derived growth factor receptor; PI3K, phosphatidylinositol 3-kinase; PSPN, persephin; PKA, protein kinase A; PKC, protein kinase C; RS or R-spine, regulatory spine; Sh1, shell residue 1; ThC, thyroid cancer; TM, transmembrane segment; VEGFR, vascular endothelial growth factor receptor.

E-mail address: rrj@brimr.org.

https://doi.org/10.1016/j.phrs.2026.108237
Received 5 May 2026; Accepted 6 May 2026
Available online 8 May 2026

all other receptor protein-tyrosine kinases because of the requirement for additional GDNF family receptor-α (GFRα) co-receptors (GFRα1/2/3/4, GFRAL) [4]. These co-receptors are anchored to the external plasma membrane by a GPI (glycosylphosphatidylinositol) anchor, and the co-receptors form binary complexes with the extracellular RET-activating ligands that in turn bind to the RET extracellular domain. The members of the GDNF family are homodimers that are linked by a disulfide bond. The GDNF dimer interacts with two GFRα complexes to form a tetramer (a dimer of dimers) that interacts with two RET receptors to form a hexameric composite containing two receptors, two co-receptors, and a ligand dimer (Fig. 1). Although there is some crossover between ligands and co-receptors, the chief ligand/co-receptor complexes consist of GDNF/GFRα1, NTRN/GFRα2, ARTN/GFRα3, PSPN/GFRα4, and GDF15/GFRAL (Table 1) [6].

Without ligand stimulation, RET exists in a nonphosphorylated dormant state. Following its stimulation, the RET receptor dimer undergoes *trans*-phosphorylation leading to its activation. Unlike that of many other receptor protein-tyrosine kinases [7], the initial activating phosphorylation sites are found outside of the activation segment [8–11]. The RET intracellular domain contains 18 tyrosine residues (Table 2). Y660 and Y697 occur within the JM segment, Y900 and Y905 occur within the activation segment, and Y1029/1062/1090/1096 occur in the C-terminal tail. Plaza-Menacho et al. discovered that Y697 and Y1062 are early phosphorylation sites and Y900 and Y905 are late phosphorylation sites [9]. These authors found that phosphorylation of Y697 within the JM segment is instrumental in promoting RET activity.

Additional receptor phosphorylation generates anchoring sites for a variety of proteins that initiate intracellular signaling by a plethora of pathways [6]. For instance, pY752 and pY928 are docking sites that lead to the activation of the JAK-STAT pathway and cell survival (Table 2). pY981 is a binding site that leads to the activation of Src and the PI3K/AKT pathway while pY1015 leads to the activation of PLCγ followed by the activation of PKC. pY1062 and pY1096 are anchoring sites that promote Ras/MAP kinase and PI3K/AKT pathway activation and cell growth, proliferation, and survival as mediated by several docking proteins including Shc1, Grb2, and Dok1/2/4/5/6. Moreover, pY905 within the activation loop is a docking site for Grb7/10 that promotes the activation of the Ras/MAP kinase pathway [6].

Alternative splicing of RET pre-mRNA produces three protein isoforms: RET9, RET44, and RET51 (Fig. 1) [6]. These differ at the C-terminus with 9, 44, and 51 unique amino acid residues following codon 1063. Although RET is unique in its mechanism of activation because of its requirement for co-receptors, it possesses an archetypal extracellular domain, a helical transmembrane segment followed by an intracellular juxtamembrane segment, a protein kinase domain, and a C-terminal tail (Fig. 2). The kinase domain includes a 21 amino-acid-residue insert (codons 823–843). The extracellular portion includes four cadherin-like domains (CD1/2/3/4) that each consists of about 110 amino acid residues [12] and a cysteine-rich segment of about 150 amino acid residues proximal to the helical transmembrane segment. RET is the only receptor protein-tyrosine kinase with cadherin-like domains. A Ca^{2+}-binding site occurs between CD2 and CD3 in the extracellular segment.

Table 1
Properties of the GDNF-GFRα and GDF15/GFRAL complexes [a].

Components	UniProtKB IDs	Residues in preproproteins	Residues in mature proteins	Selected functions
GDNF/ GFRα1	P39905/ P56159	211/465	78–211/ 25–429	Neuronal crest development
NTRN/ GFRα2	Q99748/ O00451	197/464	96–197/ 22–244	Neuronal development/ size of hematopoietic cells
ARTN/ GFRα3	Q5T4W7/ O60609	220/400	108–220/ 32–374	Neuronal survival/attracts gut hematopoietic cells
PSPN/ GFRα4	O60542/ Q9GZZ7	156/299	22–156/ 21–287	Thyroid C-cell and adrenal medulla development
GDF15/ GFRAL	Q99988/ Q6UXV0	308/394	30–194/ 19–394	Triggers an aversive response to stresses

[a] Data from https://www.uniprot.org/uniprotkb/

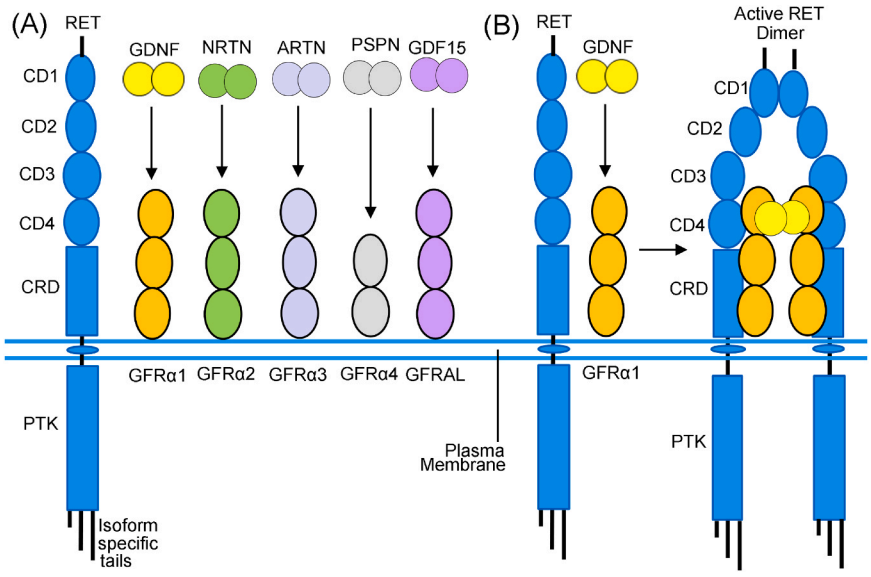

Fig. 1. (A) Activation of the RET receptor protein-tyrosine kinase by its ligands (GDNF, NTRN, ARTN, PSPN, GDF15) and its co-receptors (GFRα1/2/3/4, GFRAL). RET has three isoforms that result from alternative splicing of pre-mRNAs leading to the generation of isoform-specific tails. (B) Each RET ligand binds to corresponding co-receptors to form a ligand co-receptor dimer complex that then initiates the formation of RET dimers. Dimerization of RET leads to its activation and the subsequent phosphorylation of residues associated with enzyme activation and the formation of signal transduction docking sites. CD, cadherin-like domain; CRD, cysteine-rich domain; PTK, protein-tyrosine kinase domain.

Table 2
RET tyrosine phosphorylation sites [a].

Residue [b,c]	Location	Comments
Y687	JM	Binds PTPN1/11/13 (protein-tyrosine phosphatase non-receptor type 1/11/13) & Shp2
S696	JM	Rac1 GTPase; PKA substrate
Y752	KD, beginning of the β3-strand	Binds STAT3 to activate the JAK/STAT pathway
Y791	KD, beginning of the β4-strand	Binds STAT3
Y806	KD, hinge	Function unclear
Y809	KD, hinge	Function unclear
Y826	KID	Function unclear
Y864	KD, end of the αE-helix	Function unclear
Y900	KD, AS	Stabilizes active conformation
Y905	KD, AS	Stabilizes active conformation and binds Grb2/7/10 to activate the Ras/MAP kinase pathway
S909	AS	Autophosphorylation site required for signaling
Y928	KD, substrate binding site	Binds STAT3 to activate the JAK/STAT pathway
Y952	KD, αF-αG loop	Function unclear
Y981	KD, beginning αH-helix	Binds Sh2 domain of Src and RapGap1 (a negative regulator of Rap1 and MAP kinase)
Y1015	End of KD	Binds PLCγ leading to the activation of PKC
Y1029	CTT	Function unclear
Y1062	CTT	Binds Shc1/2, Frs2, Dok1/2/4/5/6 (Downstream of Kinases), Nck1/2, PDLIM7, Shank3 to activate PI3 kinase and Ras/MAP kinase pathways
Y1090	CTT	RET51 isoform site; function unclear
Y1096	CTT	RET51 isoform site; binds Grb2 to activate PI3 kinase and Ras/MAP kinase pathways

[a] AS, activation segment; CTT, carboxyterminal tail; KD, kinase domain; KID, kinase insert domain; JM, juxtamembrane segment; PLCγ, phospholipase C-γ.
[b] www.uniprot.org/uniprotkb/P07949/
[c] Ref. [12]

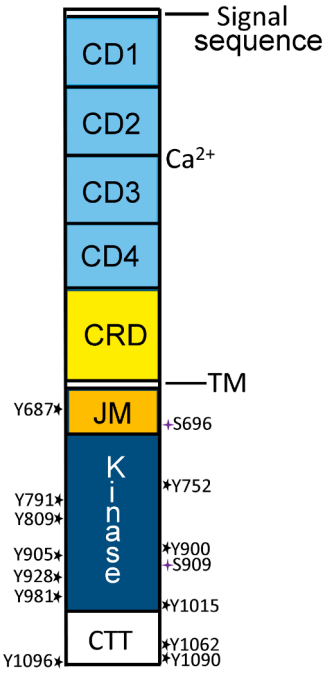

Fig. 2. Overview of the structure of RET receptor protein-tyrosine kinase. Selected serine (S) and tyrosine (Y) phosphorylation sites are depicted. CD, cadherin-like domain; CRD, cysteine-rich domain; CTT, carboxyterminal tail; JM, juxtamembrane segment; TM, transmembrane segment.

2. Properties of the RET protein-tyrosine kinase domain

2.1. Primary, secondary, and tertiary structures of the human RET catalytic domain

The RET catalytic domain contains 310 amino acid residues, which is somewhat larger than the average domain of 250–300 [13] residues owing to a kinase insert of 21 amino acid residues. The following chemical equation gives the stoichiometry of the reaction catalyzed by RET protein-tyrosine kinase:

$$MgATP^{1-} + \text{protein-tyrosine–O:H} \rightarrow \text{protein-tyrosine–O:}PO_3^{2-} + MgADP + H^+$$

Note that the phosphorylium group ($:PO_3^{2-}$) and not the phosphate ($:OPO_3^{2-}$) group is transferred from ATP to the protein substrate (I thank the late Fritz Lipmann (1899–1987) for pointing this out to me).

Using the sequences of five dozen protein-tyrosine and protein-serine/threonine kinases, Hanks and Hunter divided the structure of these enzymes into 12 domains (I-VIA, VIB-XI) [13]. RET domain I contains a glycine-rich loop (GRL) or P-loop (phosphate binding loop) with a GxGxΦG signature (^{731}GEGEFG^{736}), where Φ refers to a hydrophobic residue and is phenylalanine in the case of RET. The P-loop connects the kinase β1- and β2-strands and overlays the ATP/ADP-binding site (Fig. 3A). Owing to its role in interacting with ATP and ADP, the loop must be pliable and protein polyglycine segments exhibit this property. In active RET proteins, the P-loop has an open configuration (PDB ID: 4CKJ) while in an inactive form, the P-loop has a closed configuration (PDB ID: 4CKI) (Fig. 3B).

RET domain II has a canonical Ala-Xxx-Lys (^{756}AVK^{758}) sequence in the β3-strand and domain III has a conserved glutamate (E775) in the αC-helix that forms a salt bridge with the conserved β3-lysine while in an active protein kinase configuration. RET domain VIB has a conserved HRD signature within the catalytic loop (^{872}HRDLAARN^{879}). RET domain VII contains an ^{892}DFG^{894} sequence and domain VIII contains a ^{919}AIE^{921} sequence, which correspond to the beginning and end of the RET activation segment, respectively. Most activation segments, however, end with an APE motif. The activation segment or loop has different conformations in active and inactive protein kinase states. Protein kinase domains IX–XI consist chiefly of αE–αI helices (Fig. 3A and B).

The initial X-ray crystal structure of the protein kinase A catalytic subunit provided the requisite context for interpreting the interrelationship of the 12 domains and it has illuminated our views on the elemental biochemistry of the complete protein kinase superfamily (2CPK) [14,15]. All protein kinases, including RET, possess a small N-terminal and a large C-terminal lobe. The small lobe has five conserved β-strands (β1–5) and a critical regulatory αC-helix. The large lobe contains four conserved short strands (β6–β9) and seven helices (αD–αI and αEF) (Fig. 3A and B). All protein kinase structures that have been determined possess the typical protein kinase fold as first observed with the PKA catalytic subunit [14–16].

The K/E/D/D (Lys/Glu/Asp/Asp) tetrad occurs in all catalytically active protein kinases and these residues play significant roles during catalysis (Table 3) [16]. The lysine and glutamate are found in the N-terminal lobe and the two aspartate residues occur in the C-terminal lobe. Although ATP binds in a gap between the two lobes, there is greater interaction with the N-terminal lobe. A salt bridge linking the β3-lysine and the αC-glutamate is required for the generation of an active protein kinase, which corresponds to an "αC_{in}" conformation (Fig. 4 A). These residues in many inactive enzyme configurations fail to make electrostatic contact and constitute an inactive "αC_{out}" structure (See Refs. [16,17] for details). The αC_{in} conformation is necessary, but not sufficient, for the realization of catalytic activity.

The C-lobe interacts with the protein substrate and contains residues in the catalytic loop that play a fundamental role in the phosphoryl

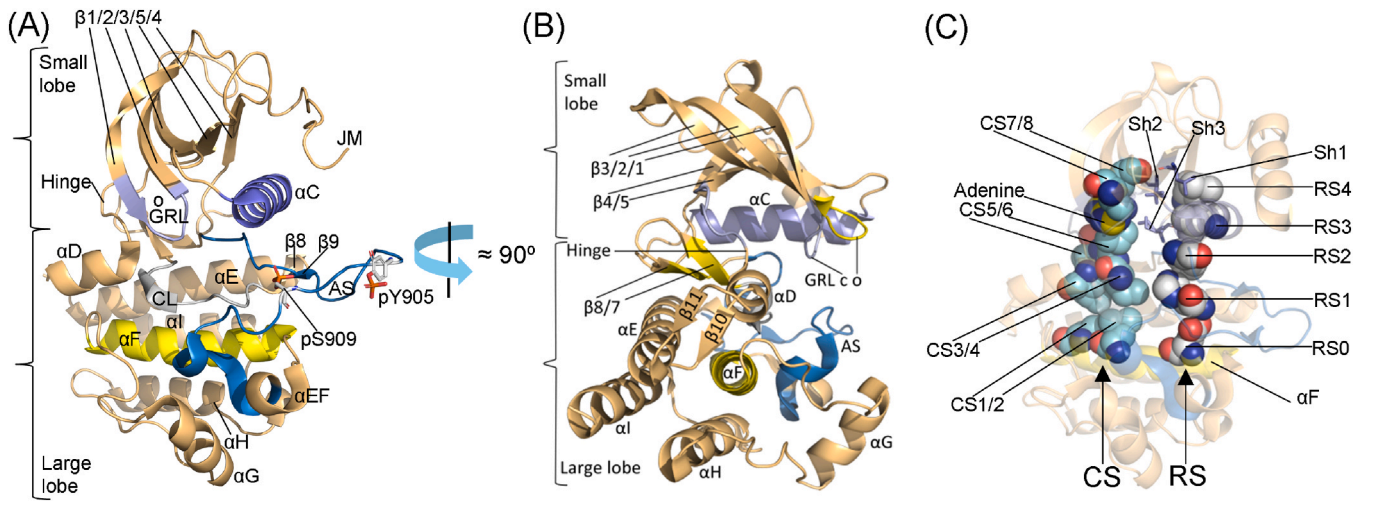

Fig. 3. Secondary and tertiary structure of the RET protein kinase domain. (A) Classical or frontal view of the protein kinase domain (PDB ID: 4CKJ). (B) Side view depicts the superposition of the closed (PDB ID: 4CKI) and open (PDB ID: 4CKJ) glycine-rich loop structures of RET. (C) RET spine and shell residues depicted for an active enzyme form (PDB ID: 4CKJ). AS, activation segment; GRL, glycine-rich loop; CS, catalytic spine; JM, juxtamembrane domain; RS, regulatory spine; Sh, Shell. c, closed conformation of the GRL; o, open conformation of the GRL. Figs. 3, 4, 9, 10 were prepared using the PyMOL Molecular Graphics System Version 2.5.4 Schrödinger, LLC.

group transfer. Moreover, two Mg^{2+} ions contribute to the catalytic cycle of most protein kinases [18] and are likely required for RET functioning. RET D892 (the DFG-D and the first D of K/E/D/D) presumably binds to Mg^{2+}(1), which in turn binds to the β- and γ-phosphates of ATP. In this active configuration, DFG-D points inward toward the active site. Furthermore, RET N879 of the catalytic loop is assumed to bind Mg^{2+}(2) (Fig. 4B), which in turn binds to the α- and γ-phosphates of ATP (not shown).

Although no X-ray crystal structure of RET with ATP/ADP is in the public domain, a phosphorylated and activated form of RET containing AMP has been described (PDB ID: 2ivt). This structure shows that the exocyclic 6-amino nitrogen of AMP hydrogen bonds with the carbonyl backbone of the first RET hinge residue (E805); the hinge connects the N- and C-terminal lobes of the protein kinase domain (Fig. 4 A). Moreover, the *N*1 nitrogen of the adenine base hydrogen bonds with the N–H group of the third hinge residue (A807). The adenine base of ATP/ADP is likely to bind similarly [16]. As detailed later, most small-molecule steady-state ATP protein kinase competitive inhibitors hydrogen bond with backbone residues of the connecting hinge. The phosphate group of pY905 within the activation segment of RET forms a salt bridge with R770 within the αC-helix and R897 and K907 within the activation loop. An additional salt bridge links R912 of the activation segment and D771 of the αC-helix (Fig. 4 A).

The activation loop binds to the protein substrate and plays a significant role in catalysis [19]. The proximal portion of the loop occurs near the N-terminus of the αC-helix and the HRD of the catalytic loop. The interfaces of these components interact hydrophobically. Phosphorylation of one or more residues within the protein kinase activation loop converts a less-active to a more-active enzyme [20], but this is not so for RET. Although RET contains two phosphorylatable tyrosine residues (Y900, Y905) within the activation loop, Plaza-Menacho et al. reported that phosphorylation and activation of RET occur after the phosphorylation of Y697 within the juxtamembrane segment and of Y1062 within the carboxyterminal tail while phosphorylation of Y900 and Y905 occurs afterwards [8,10].

Plaza-Menacho observed that activation segment S909 also undergoes phosphorylation as catalyzed by RET [10]. This finding indicates that RET is a dual specificity kinase, like MEK1/2 [21], that can catalyze the phosphorylation of both tyrosine and serine/threonine residues, a unique property for a receptor kinase. Plaza-Menacho also found that activation segment pS909 interacts with the HRD signature and facilitates both (i) regulatory-spine assembly (Section 2.2) and (ii) availability of phosphotyrosine binding modules [10]. Accordingly, pY905 is displaced and adopts a solvent-accessible configuration that can signal while ostensibly not playing an activating role.

Lemmon and Schlessinger studied the means of regulation of the receptor protein-tyrosine kinase family and most of these mechanisms involve ligand-induced (i) receptor dimer formation and subsequent protein kinase activation or (ii) activation of preformed dimers [7]. In the course of activation, one component of the dimer pair mediates the phosphorylation of activation loop tyrosine residues of the receptor partner (*trans* phosphorylation) and the phosphorylation of other protein-tyrosines that create docking sites for signal transducers that typically contain Src homology 2 (SH2) or phosphotyrosine-binding (PTB) domains [7]. Plaza-Menacho et al. found that the rate of RET phosphorylation is proportional to the enzyme concentration [8]. This result indicates that phosphorylation is intermolecular in nature and occurs in *trans*. If phosphorylation were intramolecular, the rate of RET phosphorylation would not depend on the enzyme concentration. Although activation loop phosphorylation is not required to increase catalytic activity, RET dimerization is required for enzyme activation. For RET-fusion proteins, the fusion partner promotes the dimerization that results in the subsequent activation of the protein kinase domain [22,23].

The RET catalytic loop within the C-terminal lobe contains a canonical ^{872}HRDLAARN^{879} sequence. The catalytic aspartate (D874), which is the first D of K/E/D/D, functions as a Lowry-Brönsted base and abstracts a proton from the protein-tyrosine substrate residue thereby facilitating the in-line nucleophilic attack of the tyrosyl residue onto the γ-phosphorus atom of ATP (Fig. 4B) [24]. Besides RET, the catalytic segment AAR signature occurs in many receptor protein-tyrosine kinases including VEGFR1/2/3, FGFR1/2/3/4, EGFR, Kit (the stem cell growth factor receptor), and PDGFRα/β; in contrast an RAA sequence occurs in many nonreceptor protein-tyrosine kinases such as Src [25].

2.2. *The hydrophobic spines of human RET protein kinase*

Kornev et al. examined the tertiary structures of 23 protein kinases, and they uncovered the role of several crucial amino acid residues by a local spatial pattern alignment procedure [26,27]. They identified four hydrophobic amino acid residues as components of a regulatory or R-spine [26] and eight additional residues as a catalytic or C-spine [27].

Table 3
Important human RET residues [a].

	RET residues	Comments	Hanks no.
No. of residues	1114 (RET51)/ 1072 (RET9)		
Molecular Wt (kDa)[b]	124.3/119.8		
Signal sequence	1–28		
Extracellular domain	29–635	Ligand binding	
	CD1, 28–154[c] CD2, 167–270[c] CD3, 273–387[c] CD4, 402–503[c]		
	Cys-rich 514–656	Receptor dimer formation	
Transmembrane segment	636–657	Links extracellular and intracellular domains and mediates dimer formation	
Juxtamembrane segment	658–723	Signal transduction and inhibition of basal enzyme activity	None
Juxtamembrane segment phosphorylation sites	Y687; S696	Binds PTPN1/11/13 & Shp2; GTPase activation following serine phosphorylation by PKA	None
Protein kinase domain	724–1016	Catalyzes substrate phosphorylation	
Glycine-rich loop	^{731}GEGEFG^{736}	Anchors ATP β- and γ-phosphates	I
β3-K of K/E/D/D	K757	Forms salt bridges with ATP α- and β-phosphates and with β3-K	II
αC-E, E of K/E/D/D	E775	Forms salt bridges with β3-K	III
Hinge residues	^{805}EYAKYG^{810}	Connects N- and C-lobes and hydrogen bonds with the ATP adenine and many drugs	V
Kinase insert domain	823–843	Unclear	None
Kinase domain phosphorylation sites	Y806; Y809; Y1015	Unclear; unclear; binds PLCγ	V; V; None
Catalytic loop	^{872}HRDLAARN^{879}	Plays both structural and catalytic functions	VIb
Catalytic loop HRD-D, first D of K/E/D/D	D874	Catalytic base (abstracts protein substrate proton)	VIb
Catalytic loop HRDLAARN-N	N879	Chelates Mg^{2+}(2)	VIb
AS DFG-D, second D of K/E/D/D	D892	Chelates Mg^{2+}(1)	VII
AS	D892–E921	Enzyme activity/ positions protein substrate	VII–VIII
AS phosphorylation sites	Y900; Y905	Stabilizes the AS after phosphorylation	VIII
End of AS	^{919}AIE^{921}	Interacts with the αHI loop and stabilizes the AS	VIII
C-terminal tail	1017–1114	Intracellular signaling	None
C-terminal tail phosphorylation sites	Y1062; Y1090; Y1096	Intracellular signaling; unclear; intracellular signaling	None

[a] AS, activation segment; CD, cadherin-like segment; from www.uniprot.org/uniprotkb/P07949/
[b] Molecular weight of the unprocessed and nonglycosylated precursor.
[c] From Ref. [12].

These structural spines contain residues from both the N-terminal and C-terminal lobes. The R-spine contains a residue from the important αC-helix and another from the activation loop, both of which are major elements that determine active or inactive enzyme states. The base of the R-spine within the carboxyterminal lobe anchors the catalytic loop and activation loop in an active state while the C-spine secures the adenine

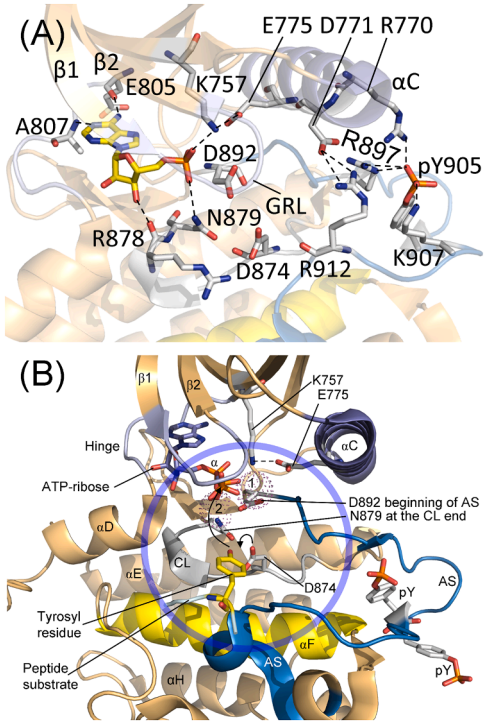

Fig. 4. (A) Interaction of AMP with the hinge residues. Prepared from PDB ID: 2ivt. The dashed lines depict polar bonds. (B) Inferred mechanism of the RET catalyzed protein kinase reaction. D874 abstracts a proton from the tyrosyl substrate allowing for its nucleophilic attack onto the γ-phosphate of ATP. The chemistry occurs within the blue circle. 1 and 2 label the two Mg^{2+} ions. AS, activation segment; GRL, glycine-rich loop; CL, catalytic loop.

base of ATP within the inter lobe crevice to facilitate catalysis. Furthermore, the precise alignment of both spines is required for the formation of an active enzyme as described for many protein-serine/threonine and protein-tyrosine kinases [28–51].

Going from the base to the apex, the protein kinase R-spine consists of the catalytic loop HRD-H, the activation loop DFG-F, an amino acid four residues carboxyterminal to the conserved αC-glutamate, and the initial amino acid of the β4-strand [26,27]. The backbone N–H of the HRD-H hydrogen bonds with an invariant side-chain aspartyl carboxylate within the hydrophobic αF-helix. Going from the bottom to the top of the spine, Meharena et al. labeled the R-spine residues as RS0, RS1, RS2, RS3, and RS4 (Fig. 3C) [52]. The R-spine of active RET is linear. The R-spine of dormant enzymes is usually nonlinear or fractured, particularly concerning the RS2 and RS3 residues. With reference to the DFG-D_{out} conformation, RS2 is displaced leftward and with respect to the αC_{out} configuration, RS3 is displaced rightward (not shown).

The catalytic spine of protein kinases includes residues from both the amino-terminal and carboxyterminal lobes. The C-spine contains the adenine base of ATP (Fig. 3C) [27]. The two residues of the N-terminal lobe that interact with the adenine moiety of ATP include a conserved valine residue in the proximal portion of the β2-strand (CS7) and the conserved alanine from the AxK signature of the β3-strand (CS8). Furthermore, a hydrophobic residue from the β7-strand (CS6) that is two residues distal to the catalytic loop interacts with the adenine moiety of ATP. Virtually all steady-state ATP-competitive protein kinase inhibitors interact with CS6. CS6 is found between two hydrophobic residues (CS4 and CS5) that are linked to the CS3 residue near the origin of the αD-helix of the large lobe (Fig. 3C). CS5/6/4 occur immediately after the catalytic loop asparagine (HRDxxxxN) so that one can easily spot these residues based upon the primary structure. Finally, CS3 and CS4 interact hydrophobically with CS1 and CS2 of the αF-helix thereby forming the complete C-spine [27]. Of importance, the hydrophobic αF-helix spans

the entire large lobe and stabilizes both spines. Both spines, moreover, play an imperative role in securing the protein kinase catalytic residues in an active configuration. CS7 and CS8 in the N-lobe make up the apex of the adenine-binding pocket while CS5/6/4 make up the base of the binding pocket. Notice that CS5/6/4 constitute the β7-strand (Fig. 3B) of the protein kinase domain.

Predicated on the results of site-directed mutagenesis, Meharena et al. characterized three shell (Sh) residues in the PKA catalytic subunit that reinforce the regulatory spine, which they labeled Sh1, Sh2, and Sh3 [52]. Sh2 corresponds to the so-called gatekeeper residue, which occurs just before the hinge-linker segment. This label portrays the part that the gatekeeper plays in controlling access to the back pocket or back cleft [53,55], which is also identified as hydrophobic pocket II (HPII) [53,54]. Compared to the identification of the canonical AxK, HRD, or DFG signatures, which is grounded upon their primary structures [13], the spines were characterized by their location in active or inactive protein kinases [26,27]. Table 4 lists the spine and shell residues of RET. As described in Section 4.2, small molecule protein kinase antagonists often interact with residues that form the C-spine (CS7/8), R-spine (RS2/3), and shell residues (S2/3), and the KLIFS-3 residue [56,57].

Modi and Dunbrack defined eight protein kinase conformations and grouped them according to the structure of the phenylalanine rotamer (plus, minus, trans) and on the Ramachandran regions (A, alpha; B, beta; L, left) of the xDF motif [58]. Their listing splits the DFG-D_{in} configuration into six clusters including BLAminus, which represents an active structure and five inactive or dormant configurations. These workers created a useful searchable and noncommercial web site (https://dunbrack.fccc.edu/kincore/) that establishes whether a given protein kinase structure corresponds to an active or inactive enzyme. We used the kincore web site to decide whether the structures of our drug-enzyme complexes correspond to an active (BLAminus) or inactive (otherwise) conformation. All RET X-ray crystal structures in the public domain portray an active protein kinase (Fig. 3A/B).

3. Thyroid cancer

3.1. Classification of thyroid cancer

Thyroid carcinoma is the most common endocrine malignancy and accounts for ≈ 2% of all cancers in the United States (Table 5) [59]. The estimated incidence in 2026 is 45,240 (13,240 male, 32,000 female) with 2320 deaths (1100 male, 1220 female). The prognosis for thyroid cancer is substantially better than that of other malignancies [60]. The estimated incidence of thyroid cancer has diminished over the last decade [38]; the reason for this is unknown.

The thyroid gland is composed mainly of follicular cells that produce thyroxine (T4) and a modest amount of tri-iodothyronine (T3). Differentiated thyroid cancers (papillary and follicular) account for about 93% of thyroid neoplasms and they are made up of two subtypes: (i) papillary thyroid cancer (PTC) and (ii) follicular thyroid cancer (FTC), which represent about 85% and 8% of cases, respectively. Both cancers originate from the thyroid follicular epithelium, and their names mirror their microscopic structure (papillae or follicles) [50]. Anaplastic thyroid cancers (ATC) are undifferentiated or dedifferentiated neoplasms that account for about 2% of cases. Medullary thyroid cancer (MTC), which is made up of parafollicular C cells, constitutes the remaining 5%. Most thyroid neoplasms (95%) stem from the follicular epithelium.

Exposure to ionizing radiation, particularly during childhood or adolescence, is a well-known risk factor for papillary thyroid carcinomas [61–63]. This cancer often arises 5–30 years after exposure, with risks particularly associated with radiotherapy or from radioactive fallout from nuclear accidents such as Chernobyl. Activating *RET* mutations were the most common mutations found in Chernobyl radiation-induced thyroid cancer. *BRAF* mutations occur in more aggressive papillary ThC. These mutations may occur concomitantly with telomerase reverse transcriptase (*TERT*) mutations [64,65]. Follicular cancer is associated with Pax8-peroxisome proliferator-activating receptor (PPAR)-γ rearrangements (≈ 30–40%) and *RAS* mutations (≈ 10–30%).

Table 4
Spine and shell residues of human RET isoforms.

Location of residues	Symbol	KLIFS No.[a]	RET9/44/51
Regulatory spine[b]			
β4-strand (N-lobe)	RS4	38	L790
C-helix (N-lobe)	RS3	28	L779
Activation loop F of DFG (C-lobe)	RS2	82	F893
Catalytic loop His (C-lobe)	RS1	68	H872
F-helix (C-lobe)	RS0	None	D933
Shell[b]			
Two residues upstream from the gatekeeper	Sh3	43	L802
Gatekeeper, end of β5-strand	Sh2	45	V804
αC-β4 back loop	Sh1	36	I788
Catalytic spine[b]			
β3-AxK motif (N-lobe)	CS8	15	A756
β2-strand (N-lobe)	CS7	11	V738
β7-strand (C-lobe)	CS6	77	L881
β7-strand (C-lobe)	CS5	78	V822
β7-strand (C-lobe)	CS4	76	I880
D-helix (C-lobe)	CS3	53	L812
F-helix (C-lobe)	CS2	None	L940
F-helix (C-lobe)	CS1	None	I944

[a] KLIFS (kinase–ligand interaction fingerprint and structure) from Refs. [56,57].
[b] From Refs. [26,27,52].

Table 5
Estimated incidence of RET-driven thyroid and lung cancers in 2026 [a].

Classification (% of total)	Incidence	No. (%) with RET mutations or fusion proteins
All thyroid cancers (100%)	45,200	7140 (15.8%)
Papillary thyroid cancer (85%)	38,400	5760 (15%)
Medullary thyroid cancer (5%)	2300	1380 (60%)
Sporadic medullary thyroid cancer (3.7%)	1700	850 (50%)
Familial medullary thyroid cancer (1.3%)	600	600 (100%)
Follicular thyroid cancer (8%)	3600	Nil
Anaplastic thyroid cancer (2%)	900	Nil
NSCLC (100%)	207,000	2000–4000 (1–2%)

[a] Ref. [38].

3.2. Treatment of thyroid cancer

3.2.1. Differentiated and undifferentiated thyroid cancer

Most people with thyroid neoplasms present with a nodule or mass in the neck [60]. Most nodules are benign and only 10–15% are found to be malignant following a biopsy. The major clinical challenge is to definitively differentiate benign from malignant disease to ensure appropriate management while avoiding unnecessary treatment. The thyroid cancer patient is generally euthyroid, both clinically and biochemically. Diagnostic radionuclide scans with I^{123} may display a cold nodule (cancer cells often appear as "cold" spots because they do not take up iodine as efficiently as healthy thyroid tissue). The diagnosis can be established preoperatively by fine needle aspiration or biopsy.

Both active surveillance and unilateral thyroid lobectomy are acceptable options for low risk papillary or papillary/follicular thyroid tumors smaller than 1 cm [60]. Total thyroidectomy was traditionally the standard of care for most thyroid cancer cases. However, thyroid lobectomy is a reasonable option in patients with low-risk papillary or follicular cancer such as those younger than 45 years of age, those with an intrathyroidal unifocal tumor, those with a tumor smaller than 4 cm, and those lacking nodal disease or extrathyroidal extension [66,67].

Total thyroidectomy remains the treatment of choice in patients with a higher risk of recurrence including a primary tumor larger than 4 cm, the presence of an extrathyroidal extension, and regional or distant metastasis [67,68]. Patients with tumors between 1 and 4 cm with risk factors such as familial differentiated thyroid cancer, prior radiation therapy to the neck area, age older than 45 years, and the occurrence of contralateral thyroid nodules often undergo total thyroidectomy to facilitate postoperative radioactive iodine (RAI) treatment [69]. The extent of a surgical resection depends upon the findings of a preoperative ultrasound scan of the neck which helps to identify cervical lymph node involvement. I^{131} is absorbed by follicular thyroid cells and, to a lesser degree, by their neoplastic counterparts. Postoperative scanning allows for the detection of residual local foci or distant disease. Since I^{131} is concentrated by follicular thyroid cells, γ-ray emission allows for the detection and localization of any residual thyroid tissue or metastases. Serial determination of thyroglobulin levels following surgery is also used to monitor the occurrence of neoplastic thyroid cells. Undetectable serum thyroglobulin levels foreshadow a low likelihood of residual disease and are a prognosticator of a better outcome.

Distant metastases occur in about 5–10% of patients with differentiated (papillary or follicular) thyroid cancer [70]. About half of these patients have an observable metastasis at the time of their initial presentation. The most common sites of tumor spread are the lungs and bone, followed by liver, brain, skin, muscle, and kidney. If the metastatic site is easily accessible and confined, surgery is the treatment of choice. In those patients with unresectable cancer or with distant metastases, a therapeutic dose of I^{131} is a treatment option [69]. Radioiodine is trapped by the thyroid follicular cells as well as their neoplastic counterparts. I^{131} is radioactive and emits both β-particles (electrons) and electromagnetic γ-rays. It decays primarily through β-emission (90%) that induces radiation toxicity and cell death and secondarily through γ-radiation (10%) that is useful for imaging. Other beta-gamma emitters that are medically important include cobalt-60 (Co^{60}) that is used for gamma knife surgery and technetium-99 (Tc^{99}) that is used for medical imaging. Total ablation of both normal and cancerous thyroid follicular cells by I^{131} improves the significance of serum thyroglobulin measurements as a marker of recurrent or metastatic disease. People with papillary ThC have an excellent prognosis with a 10-year survival exceeding 95% and those with follicular ThC have a 10-year survival ranging from 80 to over 90% [70].

Patients with follicular ThC may present with a slowly enlarging and painless thyroid nodule, but metastases to bone, lungs, brain, or liver occur more commonly than in those with papillary thyroid carcinomas [67]. The treatment for both disorders is identical, but the clinical course is less encouraging for patients with follicular ThC. In this patient cohort, the 10-year survival approaches 50% for those with early metastases and more than 90% in those without metastases.

Anaplastic thyroid carcinoma is a locally and systemically aggressive undifferentiated tumor with a dire mortality rate approaching 100% [64]. More than 90% of patients are more than 50 years of age with a female/male ratio of ≈ 2/1. Patients with this disease often present with a rapidly enlarging neck mass and symptoms of cough, dysphagia, dyspnea, or hoarseness caused by invasion of the recurrent laryngeal nerve. Therapeutic results are bleak. Owing to the aggressiveness of this malignancy, treatment is palliative. The B-Raf inhibitor dabrafenib is FDA-approved for those patients bearing a *BRAF* V600E mutation. On those rare instances lacking distant metastases at the time of diagnosis, surgery is the first-line treatment option. The median survival ranges from three to five months and the one year survival is ≈ 20% [64].

3.2.2. Medullary thyroid cancer

Medullary thyroid carcinoma (MTC) is distinct from other thyroid tumors both embryologically and clinically [71]. It arises from the neoplastic transformation of parafollicular thyroid C cells (calcitonin-secreting cells). These cells, which also secret carcinoembryonic antigen (CEA), are of neuroendocrine origin and occur in the connective tissue bordering thyroid follicles. Approximately 75% of medullary carcinomas are sporadic and 25% are hereditarily transmitted as an autosomal dominant trait (Table 5) [72]. Familial medullary thyroid carcinoma commonly occurs as a component of a multiple endocrine neoplasia syndrome (80% MEN2A and 5% MEN2B). The remaining 15% lack other endocrine gland abnormalities [73]. In MEN2A, which is generally diagnosed in the second or third decade of life, medullary ThC co-exists with a benign adrenal medullary pheochromocytoma (50% of cases) and hyperparathyroidism (20–30%) resulting from a benign parathyroid neoplasm. In MEN2B, medullary ThC can occur within the first year of life and is associated with a pheochromocytoma in approximately 50% of patients. MEN2B patients can also possess intestinal ganglioneuromas, mucosal neuromas, and marfanoid phenotypic features (long fingers, long limbs and toes, and crowded oral maxilla). MEN2B medullary carcinomas are generally more severe than those occurring in MEN2A. In the former (MEN2B), metastatic disease can occur in the first year of life. Medullary ThC is least aggressive in patients with isolated familial medullary thyroid carcinoma unrelated to MEN2A or MEN2B syndromes [73]. It is caused by inherited germline *RET* proto-oncogene mutations.

Many familial medullary thyroid cancer patients are diagnosed following genetic testing of first degree relatives of a patient known to have this malignancy [73]. In other instances, a *de novo* mutation results in a familial index case of medullary ThC. About 6% of patients with sporadic medullary ThC possess a germline *RET* mutation. Sporadic medullary thyroid carcinoma is generally a clinically mild disorder [60]. RET screening is recommended at less than six months of age for familial medullary ThC, and MEN2A screening is recommended by five years of age. The most common sites of mutation include exons 10 and 11 (C609, C611, C618, C620, C630, and C634) and RET codon mutations in exons 13, 14, 15, and 16. Lacking a familial index case, a patient may present with cardiovascular symptoms related to a pheochromocytoma or to hypercalcemia owing to a parathyroid adenoma.

Surgical excision is the first line treatment option in medullary thyroid carcinoma and is curative [71]. Total thyroidectomy, early in childhood or at the time of diagnosis, is also recommended for asymptomatic carriers [74]. Hypoparathyroidism and recurrent laryngeal nerve damage are the most frequently observed complications. For carriers of a hereditary *RET* mutation, prophylactic total thyroidectomy is based upon the specific mutation. The M918T, C634F/G/R/S/W/Y, and A883F are the highest risk mutations and others are classified as moderate risk mutations. Total thyroidectomy is recommended in patients with MEN2B in the first year of life. Children with MEN2A with high-risk *RET* mutations should have a total thyroidectomy by the age of five years. MEN2A moderate-risk *RET* mutation carriers may have prophylactic total thyroidectomy during childhood or when the calcitonin level is elevated. Historically, the management of patients with inaccessible distant metastases has been challenging and unsatisfactory. I^{131} treatment is not an option in patients with medullary ThC because C-cells are not iodine-avid.

3.3. Driver mutations and treatment options in thyroid cancer

RET point mutations have been observed in familial medullary thyroid carcinomas and multiple endocrine neoplasia (MEN2A and MEN2B) [68,74]. In contrast, RET-fusion proteins have been reported in papillary thyroid carcinoma and in non-small cell lung cancer. Most papillary thyroid carcinomas have mutations involving the genes encoding KRAS, B-Raf protein-serine/threonine kinase, or RET, ALK, or NTRK protein-tyrosine kinases [68,74]. Such mutations are mutually exclusive. Approximately one-third of these neoplasms possess a $BRAF^{V600E}$ gain-of-function mutation (which is associated with extrathyroidal extension and metastatic disease). Paracentric inversion or translocations of *NTRK1* on chromosome 1q21, which result in activated gene products, are present in 5–10% of papillary thyroid neoplasms. Under normal conditions, thyroid follicle cells lack the *RET* gene product. In

papillary thyroid tumors, however, a paracentric inversion within chromosome 10 or a reciprocal translocation between chromosomes 10 and 17 positions the protein-tyrosine kinase domain under the transcriptional control of genes that are normally expressed within the thyroid epithelium. About five dozen fusion partners of RET have been described in papillary thyroid carcinomas, but the most common of these RET fusions are CCDC6-RET and NCOA4-RET [23,70,73–76].

Unlike papillary malignancies, follicular thyroid cancer (FTC) is driven primarily by mutations in the Ras-MAP kinase pathway – most commonly (40–50%) featuring *RAS* mutations (*HRAS, NRAS, KRAS*) and *PAX8/PPARγ1* chromosomal translocations (25%) [64,70]. The PI3K/AKT is frequently activated in follicular thyroid cancer, acting as a primary driver for tumorigenesis, progression, and metastasis. Activated AKT promotes tumor cell survival and growth, which is often driven by *PTEN* loss (5%) or *PIK3CA* mutations (5%), and is associated with increased tumor invasiveness. Other significant mutations (15%) include *TERT* promoter mutations (often associated with more aggressive behavior), *EIF1AX*, and *TP53* [77]. Anaplastic thyroid carcinomas possess various molecular alterations including *TERT* (75%) promoter mutations, *RAS* mutations (20–40%), *BRAF* mutations (35%), inactivation of the *TP53* gene (70%), and effectors of the PI3K/AKT pathway [64,70,77]. Whereas the mutations in follicular and papillary thyroid cancer are mutually exclusive, those in anaplastic thyroid cancer are not. The *TERT* mutations often combine with those of *RAS* or *BRAF* and are associated with more severe outcomes.

Distant metastases to lung, bone, and soft tissues occur in about 15% of patients with follicular or papillary ThC [60]. In people with distant metastasis or nonresectable disease, I^{131} is a treatment option as long as the neoplastic cells take up the isotope. In patients with progressive disease that does not respond to standard therapies (surgery, radioiodine), the use of sorafenib and lenvatinib has been approved by the FDA (www.brimr.org/PKI/PKIs.htm) [77]. Sorafenib and lenvatinib are multikinase inhibitors that target Kit, PDGFRα/β, RET, and VEGFR1/2/3. Following the ablation of the thyroid gland, daily levothyroxine is prescribed as hormone replacement therapy and it additionally suppresses thyroid-stimulating hormone (TSH) production, which can blunt the recurrence of neoplastic disease.

As noted previously, surgery is the cornerstone of therapy for both familial and sporadic medullary thyroid carcinomas [60]. For at-risk carriers of familial *RET* mutations that are associated with severe medullary thyroid carcinomas (codon 609, 611, 618, 620, 630), prophylactic total thyroidectomy is recommended following the diagnosis. These mutations are found within the cysteine-rich extracellular segment of RET (Fig. 5). For patients with *MEN2B* mutations in codon 883 or 918, prophylactic thyroidectomy is recommended in the first year of life. Thyroidectomy can be delayed in patients with less aggressive medullary ThC with mutations involving RET codons 790, 791, 804, or 891, provided that there is close monitoring and follow-up. Selpercatinib is FDA-approved for the treatment of *RET* mutant metastatic medullary thyroid carcinoma and RET gene fusion metastatic differentiated thyroid cancer. Moreover, vandetanib has been approved for the treatment of progressive medullary thyroid carcinoma with unresectable or locally advanced disease (www.brimr.org/PKI/PKIs.htm) [77].

4. RET-fusion proteins in thyroid and lung cancer

RET-fusion proteins in thyroid cancer are oncogenic rearrangements found in 10–20% of papillary ThC patients [66,70,73,74]. The most common fusion proteins include CCDC6-RET and NCOA4-RET, which together make up about 90% of cases. These fusion proteins, along with others like TRIM24-RET, TRIM33-RET, and TGF-RET promote neoplastic growth by producing continuous, ligand-independent activation of the RET protein kinase domain. The 5′ end of a partner gene (e.g., *CCDC6*) fuses with the 3′ end of the *RET* gene, placing the RET kinase domain under the control of a constitutively active promoter, leading to continuous kinase activation. NCOA4-RET, the second most common of these fusion proteins, is often associated with faster growth, more aggressive behavior, and a higher risk of lymph node metastasis.

Lung cancer accounts for about 11% of all new neoplasms diagnosed in the United States [59]. Siegel et al. estimate that 229,410 people will develop cancer of the lung and bronchus in 2026 (118,500 women, 110,910 men) and 124,990 people will die of the disease (61,950 women, 63,040 men) [59]. About 85% of these will be NSCLC (195,000) and of these about 1–2% will be RET-fusion positive [23]. Approximately 30–40% of patients with NSCLC present with metastatic disease (Stage IV) at the time of the initial diagnosis [23]. Common early metastatic sites include the bones, brain, liver, and adrenal gland. Combination chemotherapy and immunotherapy are usually the treatment of choice for this group. Shaw et al. estimate that 1–2% of patients with NSCLC harbor RET-fusion proteins [23]. With the estimated 230,000 patients developing lung cancer in the US in 2026 and assuming that 90% of these new cases are NSCLC (207,000), the incidence of new cases of RET-fusion protein lung cancer range from about 2000–4000 per year (Table 5)

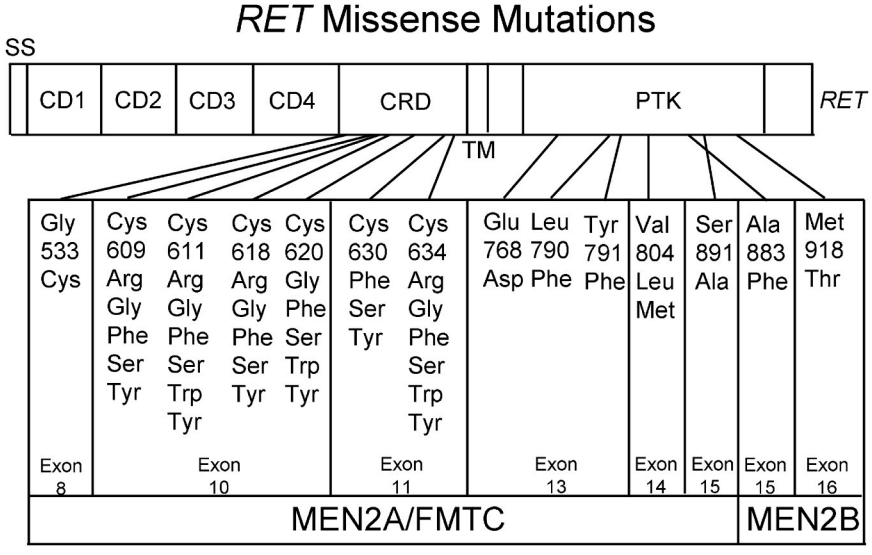

Fig. 5. RET missense mutations in MEN2A, familial medullary ThC (FMTC), and MEN2B. CD, cadherin-like domain; CRD, cysteine-rich domain; FMTC, familial medullary thyroid cancer; PTK, protein-tyrosine kinase domain; TM, transmembrane; SS, signal sequence. Adapted from Ref. [61].

The most common RET-fusion partner in NSCLC is KIF5B-RET [76]. Other RET partners are CCDC6, NCOA4, and TRIM33, which are found in both NSCLC and papillary ThC [23]. Lung cancer patients harboring RET-fusion proteins tend to be relatively young (< 60 years of age, where the median age of NSCLC onset is ≈ 70 years) with minimal or no prior history of cigarette smoking [76]. Historically, several multikinase inhibitors were used for the management of RET-fusion-protein-positive lung cancer including cabozantinib, vandetanib, ponatinib, sunitinib, and sorafenib [23,38,77]. Owing to the inhibition of multiple protein kinases, these drugs were accompanied by numerous side effects and are no longer recommended for the first-line treatment of RET-fusion NSCLC. They have been supplanted with the specific RET blockers selpercatinib (preferred) and pralsetinib [78].

5. Drugs approved for the treatment of RET-driven thyroid and lung cancer

5.1. Clinical trial summary

The FDA approved selpercatinib for the treatment of RET-fusion positive (i) NSCLC, (ii) ThC and (iii) solid tumors and RET mutant medullary ThC. Pralsetinib is approved for the treatment of RET-fusion positive (i) NSCLC and (ii) ThC (www.brimr.org/PKIs/htm). These drugs are rather specific RET blockers. The FDA also approved cabozantinib, lenvatinib, and sorafenib for the treatment of differentiated ThC (papillary and follicular) and vandetanib for the treatment of medullary ThC (Table 6). The latter four drugs are multikinase blockers often associated with serious side effects. The multikinase blocker sunitinib is used off label for the management of medullary and differentiated thyroid cancer. See Refs. [4,7,23,76,79–85] for documentation on the clinical trials that led to the approval of these drugs for the treatment of thyroid and lung cancer.

5.2. A description of protein kinase-inhibitor complexes and inhibitor-binding pockets

Based upon previous work [86–90], we divided small molecule protein kinase antagonists into seven types including reversible (Groups I, I½, II, III, IV, and V) and targeted covalent inhibitors (VI) as shown in Table 7. We separated type I½ and type II antagonists into A and B subtypes [79]. Subtype A inhibitors extend beyond the gatekeeper residue into the back cleft. In contrast, subtype B drugs fail to enter the back cleft. The potential importances of this difference, based upon preliminary findings, is that subtype A antagonists bind to their kinase target with longer residence times than subtype B inhibitors [79]. For instance, sorafenib is a type IIA VEGFR inhibitor and sunitinib is a type IIB VEGFR blocker, both of which are used for the management of differentiated ThC. The type IIA blocker has a VEGFR residence time greater than 64 min while the type IIB antagonist has a residence time of less than 2.9 min [79].

Table 7
Classification of small molecule protein kinase inhibitors [a].

Inhibitor type	Properties
I	Binds in and around the ATP-binding pocket of an active enzyme
I½ A/B	Binds in and around the ATP-binding pocket of an inactive DFG-D_{in} enzyme
I½ A	Extends into the back cleft
I½ B	Does not extend into the back cleft
II A/B	Bind in and around the ATP-binding site of an inactive DFG-D_{out} enzyme
II A	Extends into the back cleft
II B	Does not extend into the back cleft
III	Allosteric inhibitor bound next to the ATP-binding site
IV	Allosteric inhibitor bound away from the ATP-binding site
V	Bivalent inhibitor spanning two kinase domain regions
VI	Covalent inhibitor

[a] Ref. [79].

The region between the N-terminal and C-terminal protein kinase lobes is partitioned into a front cleft or front pocket, a gate area, and a back cleft. An outline depicting the location of these regons is illustrated in Fig. 6 and listed in Table 8. The back pocket (hydrophobic pocket II, or HPII) contains the gate area and its adjacent back cleft. The front cleft includes the small lobe glycine-rich loop, the hinge-linker residues that connect the small lobe to the large lobe, the adenine-binding pocket (AP), and the catalytic loop (HRD(x)$_4$N).

Type I inhibitors interact with residues in the front cleft [91–94]. The gate area includes amino acid residues from both lobes including the last three residues of the β3-strand and the first two residues of the β3-αC loop. The gate area also includes the residue directly before the activation segment (the x of xDFG) and the first four residues of the activation segment. The back cleft contains residues from the central

Table 6
Properties of selected orally effective small molecule RET inhibitors.

Name, code, trade name®	Selected targets	PubChem CID[a]	Formula	MW (Da)	D/A[b]	RET IC_{50} (nM)[c]	FDA-approved indications (year of initial approval)[d]
Pralsetinib, Blu667, Gavereto	RET	129073603	$C_{27}H_{32}FN_9O_2$	533.6	3/9	0.4	RET fusion-positive ThC; RET fusion-positive NSCLC (2020)
Selpercatinib, LY3527723, Retevmo	RET	134436906	$C_{29}H_{31}N_7O_3$	525.6	1/9	1	*RET*-mutant medullary ThC; RET fusion-positive ThC and NSCLC; other RET fusion-positive solid tumors (2020)
Vandetanib, ZD6474, Caprelsa®	RET, EGFRs, VEGFRs, Brk, Tie2, EphRs, Src family kinases	3081361	$C_{22}H_{24}BrFN_4O_2$	475.3	1/7	100	Medullary ThC (2011)
Cabozantinib, XL-184 and BMS-907351, Cometriq®	RET, VEGFR1/2/3, MET, Kit, Flt-3, Tie-2, TrkB, Axl, ROS1	25102847	$C_{28}H_{24}FN_3O_5$	501.5	2/7	5–10	RCC; HCC; differentiated ThC; pNET; epNET, extra-pancreatic neuroendocrine tumors (2012)
Lenvatinib, E7080, Lenvima®	RET, VEGFR2, FGFR1/2/3/4, PDGFRα, Kit	9823820	$C_{21}H_{19}ClN_4O_4$	426.9	3/5	1.5	Differentiated ThC refractory to radioiodine treatment; RCC (2015)
Sorafenib, BAY 43–9006, Nexavar®	RET, Raf, Kit, Flt3, VEGFR1/2/3, PDGFRβ	216239	$C_{21}H_{16}ClF_3N_4O_3$	464.8	3/7	15	RCC (2005); HCC (2007); Differentiated ThC refractory to radioiodine treatment (2013)
Sunitinib, SU-11248, Sutent®	RET, PDGFRα/β, VEGFR1/2/3, Kit, CSF-1R, Flt3	5329102	$C_{22}H_{27}FN_4O_2$	398.4	3/4	220	RCC (2006), GIST (2006), pNET (2011)

[a] www.ncbi.nlm.nih.gov/pccompound
[b] No. of hydrogen bond donors/acceptors.
[c] Refs. [77,78,83–85]
[d] GIST, gastrointestinal stromal tumor; HCC, hepatocellular carcinoma; NSCLC, non-small cell lung cancer; pNET, pancreatic neuroendocrine tumor; RCC, renal cell carcinoma, ThC, thyroid cancer.

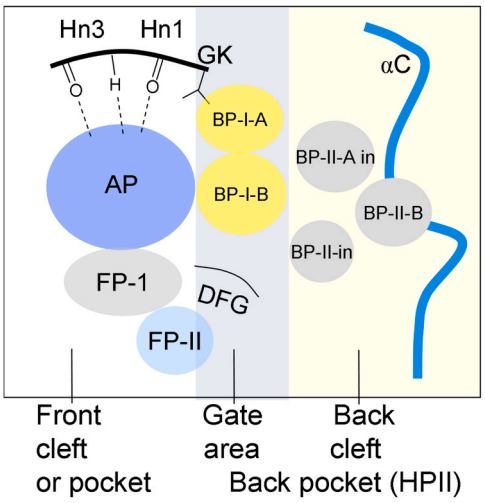

Fig. 6. Structure of the protein kinase domain drug-binding pockets. AP, adenine pocket; BP, back pocket; FP, front pocket; Hn, hinge; HP, Hydrophobic pocket II. Adapted from Refs. [54,56].

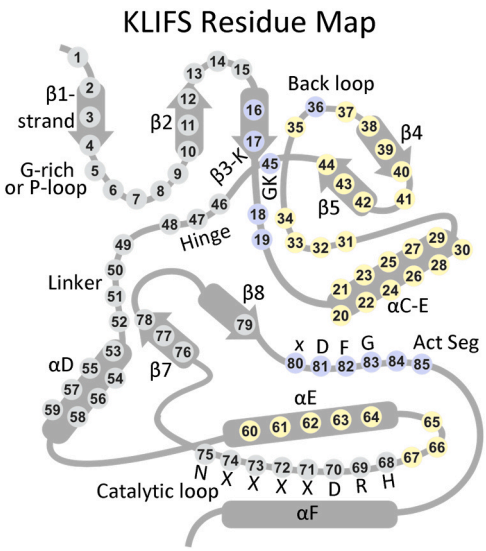

Fig. 7. The location of the KLIFS residues within a generic protein kinase domain. Act Seg, activation segment; GK, gatekeeper. Residues in gray circles are found in the front cleft; blue circles, gate area; yellow circles, back cleft.

Table 8
Location of important residues within the front cleft, gate area, and back cleft.

Description	Location	KLIFS residue no.[a]
GxGxΦG	Front cleft	4–9
β2-strand V (CS7)	Front cleft	11
β3-strand A (CS8)	Front cleft	15
HRD with DFG-D_{in}	Front cleft	68–70
HRD(x)$_4$N-N	Front cleft	75
β7-strand CS6	Front cleft	77
β3-strand K	Gate area	17
αC-β4 penultimate back loop residue	Gate area	36
Gatekeeper	Gate area	45
The x of xDFG	Gate area	80
DFG	Gate area	81–83
αC-helix E	Back cleft	24
RS3	Back cleft	28
HRD with DFG-D_{out}	Back cleft	68–70

[a] Refs. [56,57].

αC-helix along with the entire β4 and β5-strands. The back cleft also harbors the entire αE-helix and the three residues proximal to the catalytic loop HRD. Several type I½ antagonists reside in both the front cleft and a segment of the back cleft. One overall strategy in the development of small molecule protein kinase antagonists is to maximize selectivity and to minimize off-target interactions that can lead to adverse side effects; this approach is aided by evaluating drug interactions with target and nontarget proteins [17,95,96]. The creation of ligand fragments that interact with amino acids that border different pockets is a fundamental part of protein kinase inhibitor discovery with a goal of maximizing drug affinity.

Kooistra et al. [92], Kanev et al. [94] and Wu et al. et al. [95] described ligand and drug binding to about 6000 human and mouse protein kinases. Their KLIFS (kinase–ligand interaction fingerprint and structure) index encompasses an array of 85 residues occurring in each lobe that interact with various compounds; this data enables the assessment of drugs and ligands based upon their binding properties. Such information facilitates the identification of common and unique drug-protein interactions. These investigators devised a standardized amino-acid-residue numbering system that allows for the comparison of various protein kinases and their ligands. The relationship of the KLIFS terminology with the C-spine, R-spine, and shell amino-acid-residue numbering system is reviewed in Table 4 and the location of the KLIFS residues within the protein-kinase domain are illustrated in Fig. 7. These authors created a useful noncommercial and searchable web site that provides valuable information on revealing how drugs and ligands bind to their protein kinase targets (klifs.net).

5.3. *Structures of drug-RET complexes*

Selpercatinib is a pyrazolo[1,5-*a*] pyridine derivative (Fig. 8A) of RET (IC_{50} value of ~ 1 nM) that is FDA approved for the management of *RET* mutant medullary ThC and RET-fusion protein (i) ThC, (ii) NSCLC, and (iii) solid tumors (www.brimr.org/PKIs/htm). Subbiah et al. determined the X-ray crystal structure of the RET-selpercatinib complex [96] and observed that the N–H group of A807 (the third hinge residue) hydrogen bonds with the pyridine moiety of the drug (Fig. 9A). The drug interacts hydrophobically with three spine residues (CS6/7/8), one shell residue (Sh2), and the KLIFS-3 residue (Table 9). The medicine also interacts hydrophobically with ^{731}GEG^{733} and G736 of the glycine-rich loop, K737 and V738 of the β2-strand, AxK-K758 and L760 of the β3-strand, D771 and L772 of the αC-helix, V804 (the gatekeeper), and ^{805}EYAKYG^{810} of the hinge-linker segment. The drug occupies the front pocket and FP-II. The enzyme is in the active BLAminus conformation [58] and is classified as a type I antagonist [79]. See Refs. [84] for a summary of the studies that led to its FDA approval.

Pralsetinib is a pyrazole-amino-pyrimidine derivative (Fig. 8B) of RET (IC_{50} value of ~ 0.5 nM) that is FDA-approved for the treatment of RET-fusion-positive ThC and RET-fusion-positive NSCLC. Subbiah et al. determined the X-ray crystal structure of the RET-pralsetinib complex [96] and discovered that the pyrazole hydrogen bonds with E805 (the first hinge residue) and A807 (the third hinge residue). The amino group also hydrogen bonds with A807 (Fig. 9B). Like selpercatinib, pralsetinib interacts hydrophobically with three spine residues (CS6/7/8), one shell residue (Sh2) and the KLIFS-3 residue (Table 9). The agent interacts hydrophobically with ^{731}GEG^{733} and G736 of the glycine-rich loop, K737 and V738 of the β2-strand, ^{758}KML^{760} of the β3-strand, L772 of the αC-helix, V804 (the gatekeeper residue), and ^{805}EYAKYGS^{811} of the hinge-linker segment. The drug occupies the front pocket and FP-II. The enzyme is in the active BLAminus conformation [58] and is classified as a type I antagonist [79]. See Refs. [85] for a summary of the studies that led to its FDA approval.

Vandetanib (*N*-(4-bromo-2-fluorophenyl)-6-methoxy-7-((1-methylpiperidin-4-yl) methoxy) quinazolin-4-amine) (Fig. 8C) is a multikinase inhibitor that was approved by the FDA for the treatment of medullary ThC (www.brimr.org/PKI/PKIs.htm). Its IC_{50} for RET is about 17 nM

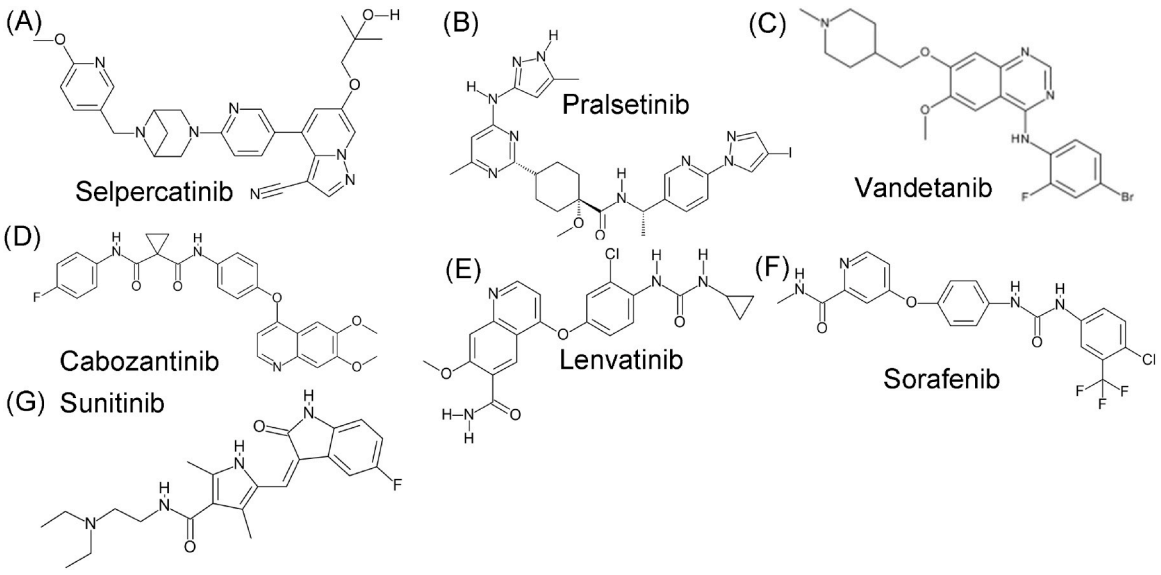

Fig. 8. Structures of RET specific (A, B) and nonspecific (C–G) blockers.

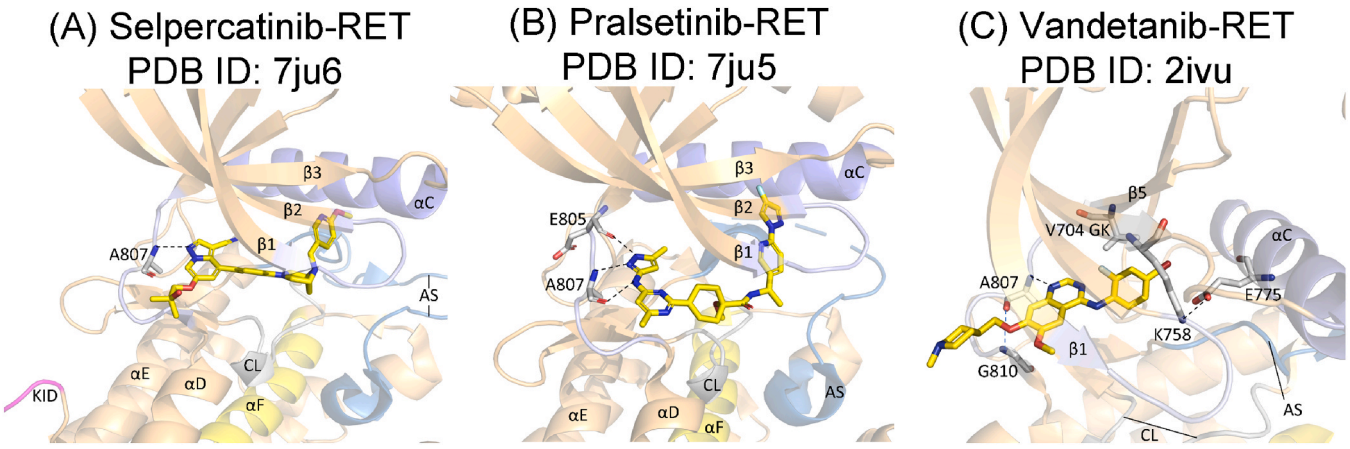

Fig. 9. Structures of RET-drug complexes. The dashed lines depict polar bonds. The carbon atoms of the drug are colored yellow and those of RET are colored gray. AS, activation segment; CL, catalytic loop.

Table 9
Drug-RET hydrophobic (Φ) interactions based upon their common KLIFS residue numbers [a].

	PDB ID ↓	RS1	RS2	RS3	RS4	Sh1	Sh2	Sh3	CS5	CS6	CS7	CS8	KLIFS-3[b]	C[c]/D[d]	Drug-binding pockets[e]
KLIFS no. →		68	82	28	38	36	45	43	76	77	11	15	3		
Drug-enzyme ↓															
Selpercatinib-RET	7ju6						Φ			Φ	Φ	Φ	Φ	in/in	F, FP-II
Pralsetinib-RET	7ju5						Φ			Φ	Φ	Φ	Φ	in/in	F, FP-II
Vandetanib-RET	2ivu			Φ		Φ	Φ	Φ		Φ	Φ	Φ	Φ	in/in	F, G, BP-I-A/B

[a] From klifs.net
[b] KLIFS-3, kinase-ligand interaction fingerprint and structure residue-3
[c] $\alpha C_{in/out}$
[d] DFG-$D_{in/out}$
[e] Refs. [54,56] and Fig. 6.

and that for VEGFR2 is about 6 nM. Knowles et al. determined the X-ray crystal structure of the RET-vandetanib complex [97]. They observed that the *N*1 of the quinazoline group hydrogen bonds with the N–H group of A807 (the third hinge residue) (Fig. 9C). They also found that the drug interacts hydrophobically with four spine residues (CS6/7/8, RS3), three shell residues (Sh1/2/3), and the KLIFS-3 residue (Table 9). It also interacts hydrophobically with V757 and AxK-K758 within the β3-strand, I788 of the back loop, L802 of the β5-strand, and ^{805}EYAKYG^{810} within the hinge-linker segment. The compound is found in the front pocket, gate area, and BP-I-A/B of an enzyme in the active state (BLAminus) [58] and is accordingly classified as a type I inhibitor [79].

6. *RET* point mutations

Activating *RET* mutations occurring within the extracellular

cysteine-rich domain have been discovered in patients with MEN2A and familial medullary ThC [4,61–63,73,76,77,98,99]. Owing to the mutation of cysteine to another amino acid residue, disruption of intramolecular disulfide bridges results, leading to the formation of intermolecular covalent disulfide bonds (not the physiological intramolecular bonds) that produce ligand-independent dimerization and RET activation. Three substitutions involve noncysteine residues (G533C, D631Y, and K666E), but it is unclear how these mutations lead to activation of RET activity. Activating *RET* mutations within the protein kinase domain have been discovered in patients with MEN2B and in familial medullary ThC. These mutations and those that confer drug resistance are listed in Table 10.

The location of the RET protein kinase domain mutations is depicted in Fig. 10. The more challenging clinical mutations include codons 883 and 918. These patients should have a prophylactic thyroidectomy during the first year of life or at the time of diagnosis [60]. The codon 883 mutation (A883F) is located after the catalytic loop and this mutation enhances ligand-independent catalysis. The *RET* M918T mutation generates the most aggressive clinical phenotype and is the most transforming of all *RET* mutants in cultured cells [77]. This mutation is located near the end of the activation loop and the protein-substrate binding site and it may modify substrate affinity. Gujral et al. reported that the M918T mutant was more highly phosphorylated in response to growth factor stimulation in cell culture as compared with the wildtype enzyme [100]. Moreover, they reported that the mutation decreases autoinhibition by the activation loop. They also found that the mutation reduced the ATP K_m from 188 to 105 μM while its K_d decreased more than an order of magnitude from 192 to 15.3 μM. These data indicate that ATP in this mutant is better able to block drug binding to the ATP active site. We encounter the situation where a mutation 20 Å from the ATP-binding site alters nucleotide binding. Moreover, these workers found evidence that the M918T mutant dimerizes more facilely than the wildtype protein. Consequently, Gujral et al. inferred that multiple diverse, but complementary, mechanisms lead to the activation of the M918T mutant [100]

The S904 mutation involves the activation segment and its conversion to phenylalanine stabilizes the activation loop in an active conformation, enhances enzyme affinity for ATP during catalysis, thus making kinase inhibitors less effective. Less-consequential low-risk mutations include codons 768, 790, 791, 804, and 891. Surgery on patients with these mutations can be delayed until after five to ten years of age provided that they and their calcitonin levels are carefully monitored [101]. The codon E768D mutation is found four residues into the αC-helix. The carboxyl group of E768 hydrogen bonds with the S765 N–H group at the beginning of the αC-helix, but D768 is incapable of forming this bond. Furthermore, E768 forms a salt bridge with K761, but D768 is too short to form this bond. These two electrostatic bonds in the wildtype protein (E768) may produce an inactive enzyme configuration while their absence (D768) may foster the active state. The L790F or Y791F mutation is located in the proximal β4-strand. L790 is spinal residue RS4 and its mutation to phenylalanine may strengthen the spine. The mutation of the adjacent Y791F may also modify the strength and stability of the R-spine. S891 (the x of xDFG) is proximal to the activation segment and the –OH group of S891 makes electrostatic contact with the DFG-D892 side chain and its N–H group. An alanine at this position cannot make such interactions and this failure may promote the activation of RET catalytic activity.

Loss-of-function *RET* mutations result in Hirschsprung disease, a developmental abnormality of the enteric nervous system [61]. This congenital malformation is associated with aganglionosis of the gastrointestinal tract resulting in severe constipation or intestinal obstruction owing to missing nerve cells in the intestine. Hirschsprung disease is expected to occur in about 720 babies in the United States in 2026 (about 1 per 5000 live births) and most cases (80%) are localized to the rectosigmoid colon. Signs and symptoms include the failure to pass the first stool within 48 h of birth, a swollen abdomen, vomiting,

Table 10
Selected *RET* point mutations occurring in thyroid cancer, NSCLC, and Hirschsprung disease [a,b].

Mutations in the extracellular cysteine-rich segment		Protein kinase domain mutations	
Mutation	Comments	Mutation	Location; comments
Exon 8 G533C	Rare germline mutation associated with familial medullary ThC and MEN2A	*Exon 13* L730I/V	Proximal to G-rich loop; resistance to vandetanib, cabozantinib, and pralsetinib, but not selpercatinib
Exon 10 C609F/G/R/S/Y	Rare germline mutation associated with familial medullary ThC, MEN2A, and HD	*Exon 13* E768D	Fourth residue of the αC-helix; this mutation yields familial medullary ThC (a form of MEN2) and is characterized by a less aggressive clinical course, later age of onset, and incomplete penetrance
Exon 10 C611F/G/S/Y/W	Familial medullary ThC and MEN2A	*Exon 13* L790F (RS4)	Beginning of the β4-strand; low risk familial medullary ThC and MEN2A
Exon 10 C618F/R/S	Familial medullary ThC, MEN2A, and HD	*Exon 13* Y791F	Second residue of the β4-strand; mutation of questionable significance for medullary ThC, familial medullary ThC, and MEN2A
Exon 10 C620F/R/S	MEN2A and HD	*Exon 14* V804M/L (Sh2)	Gatekeeper residue leading to monomeric activation; common in familial medullary ThC and MEN2A and may lead to drug resistance to vandetanib and cabozantinib, but not selpercatinib or pralsetinib
Exon 11 C630R/Y	Medullary ThC, familial medullary ThC, and MEN2A	*Exon 14* Y806N/C/S	Hinge residue; selpercatinib or pralsetinib drug resistance following treatment of medullary ThC and NSCLC
Exon 11 D631Y	Medullary ThC and MEN2A	*Exon 15* G810S/A/C/D/R	Linker; selpercatinib or pralsetinib drug resistance following treatment of medullary ThC and NSCLC
Exon 11 C634/R/Y/S/W/G/F/A; most common	Familial medullary ThC, MEN2A	*Exon 15* V871I	Proximal to catalytic loop; drug resistance to cabozantinib
Exon 11 K666N/E	Familial medullary ThC, MEN2A	*Exon 15* A883F/T	Last residue of the β7-strand; aggressive MEN2B
		Exon 15 S891A	Between the β8-strand and activation segment; associated with familial medullary ThC and MEN2A
		Exon 16 M918T	End of the activation segment leading to monomeric activation; most common mutation in sporadic medullary ThC (95% of cases) and common in MEN2B – aggressive disease responds to selpercatinib or pralsetinib

[a] Data from Ref. [4,61–63,73,76,77,98,99].
[b] HD, Hirschsprung disease; MEN, multiple endocrine neoplasia; NSCLC, non-small cell lung cancer; ThC, thyroid cancer

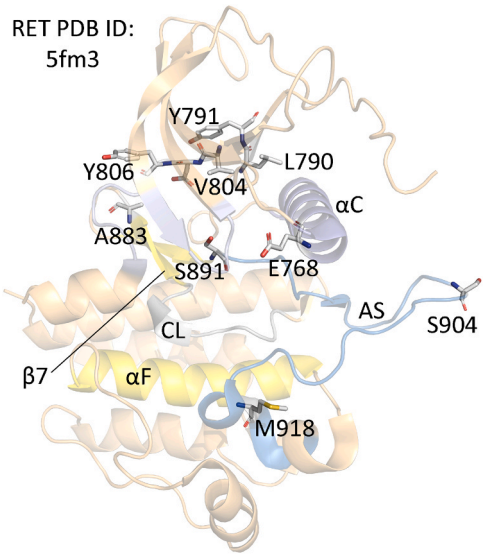

Fig. 10. Location of activating *RET* protein-tyrosine kinase point mutations. Y806, second hinge residue; A883, distal to the β-7 stramd; V804, gatekeeper; L790, RS4; S891, the x of xDFG. AS, activation segment; CL, catalytic loop.

and chronic constipation, usually diagnosed in newborns. *RET* mutations account for about 50% of familial and 10%–20% of sporadic cases. A variety of missense, nonsense, and frameshift mutations have been identified in the four cadherin-like domains, the cysteine-rich domain, the kinase domain, and the C-terminal tail. Furthermore, *RET* mutations in non-coding sequences, including the promoter/enhancer regions, result in aberrant regulation of *RET* expression. Mutations corresponding to the extracellular domain impair cell surface expression owing to protein misfolding and those corresponding to the kinase domain result in complete or partial impairment of kinase activity. Hirschsprung disease is treated primarily through surgery to remove the dysfunctional, nerve-lacking segment of the colon, allowing normal bowel movements. Most surgeries, usually performed in the first one to six months of life, are performed laparoscopically. See Ref. [61] for a list of about 20 mutations associated with Hirschsprung disease.

7. Clinical outcomes in response to RET inhibitors

The clinical success in response to RET-directed therapies was historically not as robust as those achieved with other targeted therapies aimed at other oncogenic drivers of solid tumors including ALK, B-Raf, EGFR, and ROS1 [76]. Vandetanib is approved for the treatment of medullary ThC and cabozantinib, lenvatinib, and sorafenib (Fig. 8) are approved for the treatment of differentiated thyroid cancer (papillary and follicular). These multikinase antagonists were approved regardless of the *RET* mutation status. The modest response garnered by these multikinase inhibitors is related to the parallel inhibition of VEGFR2, which limits the permissible dosage [76]. For example, at clinically achievable concentrations, cabozantinib and vandetanib are more effective inhibitors of VEGFR2 than they are of RET. Selpercatinib is approved for the management of *RET* mutant medullary ThC, RET-fusion-positive (i) ThC, (ii) NSCLC and (iii) other RET-fusion-positive solid tumors. Pralsetinib is approved for the treatment of RET-fusion-positive ThC and RET-fusion-positive NSCLC (www.brimr.org/PKI/PKIs.htm). The latter two drugs are specific RET blockers and are associated with fewer untoward side effects than the multikinase blockers.

As noted by Winer and colleagues "Biologically, the cancer cell is notoriously wily; each time we throw an obstacle in its path, it finds an alternate route that must then be blocked" [102]. L730I/V exon 13 mutations confer resistance to vandetanib, cabozantinib, and pralsetinib, but not selpercatinib (Table 10). The V804M/L exon 14 gatekeeper mutations lead to vandetanib and cabozantinib resistance, but not to that of selpercatinib or pralsetinib. The exon 14 Y806N/C/S mutations, the exon 15 G810S/A/C/D/R mutations, and the exon 15 V871I mutation lead to the resistance of selpercatinib and pralsetinib. The management of these resistant mutations is undergoing current evaluation. The activation of bypass pathways is a probable mechanism for the development of selected cases of acquired resistance following specific RET inhibitor treatment [103].

8. Epilogue

Dysregulation of protein kinases plays an essential role in the pathogenesis of autoimmune, inflammatory, nervous system disorders, cancer, and other maladies. Consequently, this enzyme family has developed into one of the most important drug targets over the past 25 years [16,104–107]. The development of therapeutic protein kinase antagonists accelerated in 2001 after the FDA approval of imatinib for the treatment of chronic myelogenous leukemia. Owing to their role in many aspects of cellular signaling, a much wider range of diseases should be amenable to treatments with protein kinase antagonists [108], and more than 400 protein kinase inhibitors are in various stages of clinical development worldwide. Accordingly, we can expect future advances in clinical effectiveness and the subsequent approval of additional drugs targeting (i) more protein kinases, (ii) neurodegenerative diseases (Alzheimer disease, amyotrophic lateral sclerosis, Huntington disease, Parkinson disease), (iii) cardiovascular diseases (hypertension, cerebral vasospasm, heart failure, cardiac ischemia), and (iv) diabetic retinopathy [31,109–112].

Only about three dozen protein kinase drug targets within a family of more than 500 enzymes are considered in the management of neoplastic and immune disorders (www.brimr.org/PKIs/htm). Most kinase inhibitors (≈ 85) are prescribed for the treatment of neoplasms including carcinomas, leukemias, and lymphomas. The FDA has approved 94 small molecule protein kinase antagonists that target about 25 different protein kinases in the treatment of various disorders (www.brimr.org/PKI/PKIs.htm). See Ref. [113] for a summary of the molecular weights, number of hydrogen bond donors/acceptors, ligand efficiencies, lipophilic efficiencies, polar surface areas, and solubilities of all 94 FDA-approved small molecule protein kinase inhibitors including the specific and nonspecific RET inhibitors included in this review. When PI3 kinase (an atypical protein kinase) blockers are added, a total of 99 of these medicines have been approved by the FDA [107]. Ninety-four of these drugs are orally effective including the drugs examined in this review.

The RET signaling pathway participates in the pathogenesis of thyroid, lung, and MEN2 neoplasms. MEN2 associated tumors include medullary ThC, pheochromocytoma, and parathyroid hyperplasia. In contrast, MEN1 associated abnormalities include the classical triad of primary hyperparathyroidism (100%), anterior pituitary adenomas (40%), and pancreatic neuroendocrine tumors (40%) [114,115]. The pancreatic neuroendocrine tumors include those secreting gastrin leading to peptic ulcers (Zollinger-Ellison syndrome) or insulin-secreting tumors leading to hypoglycemia. MEN1 patients may also develop bronchopulmonary and thymic neuroendocrine tumors and adrenal adenomas. The median age at the time of diagnosis of this uncommon disorder is 31 years. MEN1 is an autosomal dominant disorder resulting from mutations in *MEN1*, a tumor-suppressor gene encoding the menin scaffold protein that participates in the negative regulation of the cell cycle. This disease results from decreased menin activity owing to under expression or mutation in these tumors. Nearly 100 *MEN1* mutations throughout the sequence of 610 amino acid residues have been described (https://www.uniprot.org/uniprotkb/O00255/entry). These patients may present with kidney stones related to elevated Ca^{2+} levels owing to hyperparathyroidism, stomach ulcers secondary to pancreatic gastrin-producing tumors, acromegaly resulting from excess growth

hormone production by the anterior pituitary, or Cushing disease (hyperadrenocorticism) ensuing from excess ACTH production by the anterior pituitary.

The MEN1 tumors are usually benign, although they may become malignant. MEN1 is clinically challenging owing to its genetic heterogeneity, lack of genotype-phenotype correspondence, variable penetrance, and the need for lifelong surveillance [114,115]. Patients with hyperparathyroidism and pancreatic insulinoma are treated surgically, and those with Zollinger-Ellison syndrome are treated with proton-pump inhibitors. Patients with pituitary adenomas can be treated with transsphenoidal surgery, stereotactic radiation therapy (gamma knife), or external beam radiation therapy. Other management options include dopamine agonists (cabergoline or bromocriptine) for prolactinomas, somatostatin analogs (octreotide, lanreotide) or growth hormone receptor antagonists (pegvisomant) for patients with acromegaly, or adrenostatic medications like ketoconazole or mifepristone to control cortisol levels in patients with Cushing disease. Sunitinib (a multikinase and VEGFR blocker) and everolimus (an mTOR inhibitor) are targeted agents used for the treatment of MEN1-related neuroendocrine tumors.

In conclusion, selective RET antagonists have transformed the treatment landscape for RET-driven neoplasms and advances in molecular medicine have significantly improved clinical outcomes. RET inhibitors are precise, safe, orally effective, and convenient. Since they are prescribed to patients whose cancers are fueled by RET alterations, patients experience fewer side effects with better results when compared to cytotoxic chemotherapy. However, resistance to targeted therapies represents a formidable challenge, requiring continuous innovation in RET-targeted therapies. The use of immune checkpoint inhibitors as used in breast, kidney, and lung cancers [116–118] represents a possible treatment for RET-inhibitor-resistant tumors. We are still in the early years of the saga of protein kinase inhibitor development and 2025 was a banner year with the FDA approval of ten protein kinase antagonists (www.brimr.org/PKI/PKIs.htm).

CRediT authorship contribution statement

Robert Roskoski: Conceptualization, Writing – original draft, Writing – review & editing.

Declaration of Competing Interest

The author is unaware of any affiliations, memberships, or financial holdings that might be perceived as affecting the objectivity of this article.

Acknowledgment

The colored figures in this paper were checked to ensure that their perception was accurately conveyed to colorblind readers [119]. We thank Laura M. Roskoski for providing editorial and bibliographic assistance. We thank Josie Rudnicki and Jasper Martinsek for their help in preparing the figures and Pasha Brezina and WS Sheppard for their help in structural analyses. We also thank Dr. AJ Kooistra for providing Fig. 7.

Data availability

No data was used for the research described in the article.

References

[1] M. Takahashi, J. Ritz, G.M. Cooper, Activation of a novel human transforming gene, ret, by DNA rearrangement, Cell 42 (1985) 581–588, https://doi.org/10.1016/0092-8674(85)90115-1.
[2] Y. Ishizaka, F. Itoh, T. Tahira, I. Ikeda, T. Sugimura, J. Tucker, A. Fertitta, A. V. Carrano, M. Nagao, Human ret proto-oncogene mapped to chromosome 10q11.2, Oncogene 4 (1989) 1519–1521.
[3] P. Durbec, C.V. Marcos-Gutierrez, C. Kilkenny, M. Grigoriou, K. Wartiowaara, P. Suvanto, D. Smith, B. Ponder, F. Costantini, M. Saarma, H. Sariola,, V. Pachnis, GDNF signalling through the Ret receptor tyrosine kinase, Nature 381 (1996) 789–793, https://doi.org/10.1038/381789a0.
[4] D. Salvatore, M. Santoro, M. Schlumberger, The importance of the RET gene in thyroid cancer and therapeutic implications, Nat. Rev. Endocrinol. 17 (2021) 296–306, https://doi.org/10.1038/s41574-021-00470-9.
[5] G. Manning, D.B. Whyte, R. Martinez, T. Hunter, S. Sudarsanam, The protein kinase complement of the human genome, Science 298 (2002) 1912–1934, https://doi.org/10.1126/science.1075762.
[6] S. Streit, A. Dweik, A. Mahtab, S. Ali, A. Khan, M. Salzberg, RET signaling pathway in human cancer: oncogenic mechanisms, selective inhibitors, and emerging resistance strategies, Int. J. Mol. Sci. 27 (2026) 3180, https://doi.org/10.3390/ijms27073180.
[7] M.A. Lemmon, J. Schlessinger, Cell signaling by receptor tyrosine kinases, Cell 141 (2010) 1117–1134, https://doi.org/10.1016/j.cell.2010.06.011.
[8] I. Plaza-Menacho, K. Barnouin, K. Goodman, R.J. Martínez-Torres, A. Borg, J. Murray-Rust, S. Mouilleron, P. Knowles, N.Q. McDonald, Oncogenic RET kinase domain mutations perturb the autophosphorylation trajectory by enhancing substrate presentation in trans, Mol. Cell 6 (2014) 738–751, https://doi.org/10.1016/j.molcel.2014.01.015.
[9] I. Plaza-Menacho, L. Mologni, N.Q. McDonald, Mechanisms of RET signaling in cancer: current and future implications for targeted therapy, Cell. Signal. 26 (2014) 1743–1752, https://doi.org/10.1016/j.cellsig.2014.03.032.
[10] I. Plaza-Menacho, K. Barnouin, R. Barry, A. Borg, M. Orme, R. Chauhan, S. Mouilleron, R.J. Martínez-Torres, P. Meier, N.Q. McDonald, RET Functions as a dual-specificity kinase that requires allosteric inputs from juxtamembrane elements, Cell Rep. 17 (2016) 3319–3332, https://doi.org/10.1016/j.celrep.2016.11.061.
[11] Y. Kawamoto, K. Takeda, Y. Okuno, Y. Yamakawa, Y. Ito, R. Taguchi, M. Kato, H. Suzuki, M. Takahashi, I. Nakashima, Identification of RET autophosphorylation sites by mass spectrometry, J. Biol. Chem. 279 (2004) 14213–14224, https://doi.org/10.1074/jbc.M312600200.
[12] J. Anders, S. Kjar, C.F. Ibáñez, Molecular modeling of the extracellular domain of the RET receptor tyrosine kinase reveals multiple cadherin-like domains and a calcium-binding site, J. Biol. Chem. 276 (2001) 35808–35817, https://doi.org/10.1074/jbc.M104968200.
[13] S.K. Hanks, T. Hunter, Protein kinases 6. The eukaryotic protein kinase superfamily: kinase (catalytic) domain structure and classification, FASEB J. 9 (1995) 576–596.
[14] D.R. Knighton, J.H. Zheng, L.F. Ten Eyck, V.A. Ashford, N.H. Xuong, S.S. Taylor, J.M. Sowadski, Crystal structure of the catalytic subunit of cyclic adenosine monophosphate-dependent protein kinase, Science 253 (1991) 407–414, https://doi.org/10.1126/science.1862342.
[15] D.R. Knighton, J.H. Zheng, L.F. Ten Eyck, N.H. Xuong, S.S. Taylor, J.M. Sowadski, Structure of a peptide inhibitor bound to the catalytic subunit of cyclic adenosine monophosphate-dependent protein kinase, Science 253 (1991) 414–420, https://doi.org/10.1126/science.1862342.
[16] R. Roskoski Jr, A historical overview of protein kinases and their targeted small molecule inhibitors, Pharm. Res. 100 (2015) 1–23, https://doi.org/10.1016/j.phrs.2015.07.010.
[17] D. Bajusz, G.G. Ferenczy, G.M. Keser, Structure-based virtual screening approaches in kinase-directed drug discovery, Curr. Top. Med. Chem. 17 (2017) 2235–2259, https://doi.org/10.2174/1568026617666170224121313.
[18] R. Roskoski Jr, Src protein-tyrosine kinase structure, mechanism, and small molecule inhibitors, Pharm. Res. 94 (2015) 9–25, https://doi.org/10.1016/j.phrs.2015.01.003.
[19] S.S. Taylor, M.M. Keshwani, J.M. Steichen, A.P. Kornev, Evolution of the eukaryotic protein kinases as dynamic molecular switches, Philos. Trans. R. Soc. Lond. B Biol. Sci. 367 (2012) 2517–2528, https://doi.org/10.1016/j.bbapap.2013.03.007.
[20] B. Nolen, S. Taylor, G. Ghosh, Regulation of protein kinases; controlling activity through activation segment conformation, Mol. Cell 15 (2004) 661–675, https://doi.org/10.1016/j.molcel.2004.08.024.
[21] R. Roskoski Jr., MEK1/2 dual-specificity protein kinases: structure and regulation, Biochem. Biophys. Res. Commun. 417 (2012) 5–10, https://doi.org/10.1016/j.bbrc.2011.11.145.
[22] J.F. Gainor, A.T. Shaw, Novel targets in non-small cell lung cancer: ROS1 and RET fusions, Oncologist 18 (2013) 865–875, https://doi.org/10.1634/theoncologist.2013-0095.
[23] A.T. Shaw, P.P. Hsu, M.M. Awad, J.A. Engelman, Tyrosine kinase gene rearrangements in epithelial malignancies, Nat. Rev. Cancer 13 (2013) 772–787, https://doi.org/10.1038/nrc3612.
[24] J. Zhou, J.A. Adams, Participation of ADP dissociation in the rate-determining step in cAMP-dependent protein kinase, Biochemistry 36 (1997) 15733–15738, https://doi.org/10.1021/bi971438n.
[25] S.K. Hanks, A.M. Quinn, T. Hunter, The protein kinase family: conserved features and deduced phylogeny of the catalytic domains, Science 241 (1988) 42–52, https://doi.org/10.1126/science.3291115.
[26] A.P. Kornev, N.M. Haste, S.S. Taylor, L.F. Eyck, Surface comparison of active and inactive protein kinases identifies a conserved activation mechanism, Proc. Natl. Acad. Sci. 103 (2006) 17783–17788, https://doi.org/10.1073/pnas.0607656103.
[27] A.P. Kornev, S.S. Taylor, L.F. Ten Eyck, A helix scaffold for the assembly of active protein kinases, Proc. Natl. Acad. Sci. 105 (2008) 14377–14382, https://doi.org/10.1073/pnas.0807988105.

[28] R. Roskoski Jr, The ErbB/HER family of protein-tyrosine kinases and cancer, Pharm. Res. 79 (2014) 34–74, https://doi.org/10.1016/j.phrs.2013.11.002.
[29] R. Roskoski Jr, ErbB/HER protein-tyrosine kinases: Structure and small molecule inhibitors, Pharm. Res. 87 (2014) 42–59, https://doi.org/10.1016/j.phrs.2014.06.001.
[30] R. Roskoski Jr, Small molecule inhibitors targeting the EGFR/ErbB family of protein-tyrosine kinases in human cancers, Pharm. Res. 139 (2019) 395–411, https://doi.org/10.1016/j.phrs.2018.11.014.
[31] R. Roskoski Jr, Vascular endothelial cells and angiogenesis, Pharm. Res. 221 (2025) 107983, https://doi.org/10.1016/j.phrs.2025.107983.
[32] R. Roskoski Jr, Anaplastic lymphoma kinase (ALK) inhibitors in the treatment of ALK-driven lung cancers, Pharm. Res. 117 (2017) 343–356, https://doi.org/10.1016/j.phrs.2017.01.007.
[33] R. Roskoski Jr, Properties of FDA-approved small molecule protein kinase inhibitors: A 2025 update, Pharmacol. Res. 216 (2025) 107723, https://doi.org/10.1016/j.phrs.2025.107723.
[34] R. Roskoski Jr, The preclinical profile of crizotinib in the treatment of non-small cell lung cancer and other neoplastic disorders, Expert Opin. Drug Dis. 8 (2013) 1165–1179, https://doi.org/10.1517/17460441.2013.813015.
[35] R. Roskoski Jr, Hydrophobic and polar interactions of FDA-approved small molecule protein kinase inhibitors with their target enzymes, Pharm. Res. 169 (2021) 105660, https://doi.org/10.1016/j.phrs.2021.105660.
[36] R. Roskoski Jr, The role of fibroblast growth factor receptor (FGFR) protein-tyrosine kinase inhibitors in the treatment of cancers including those of the urinary bladder, Pharm. Res. 151 (2020) 104567, https://doi.org/10.1016/j.phrs.2019.104567.
[37] R. Roskoski Jr, The role of small molecule platelet-derived growth factor receptor (PDGFR) inhibitors in the treatment of neoplastic disorders, Pharm. Res. 129 (2018) 65–83, https://doi.org/10.1016/j.phrs.2018.01.021.
[38] R. Roskoski Jr, A. Sadeghi-Nejad, Role of RET protein-tyrosine kinase inhibitors in the treatment RET-driven thyroid and lung cancers, Pharm. Res. 128 (2018) 1–17, https://doi.org/10.1016/j.phrs.2017.12.021.
[39] R. Roskoski Jr, The role of small molecule Kit protein-tyrosine kinase inhibitors in the treatment of neoplastic disorders, Pharm. Res. 133 (2018) 35–52, https://doi.org/10.1016/j.phrs.2018.04.020.
[40] R. Roskoski Jr, The role of small molecule Flt3 receptor protein-tyrosine kinase inhibitors in the treatment of Flt3-positive acute myelogenous leukemias, Pharm. Res. 155 (2020) 104725, https://doi.org/10.1016/j.phrs.2020.104725.
[41] R. Roskoski Jr, ROS1 protein-tyrosine kinase inhibitors in the treatment of ROS1 fusion protein-driven non-small cell lung cancers, Pharm. Res. 121 (2017) 202–212, https://doi.org/10.1016/j.phrs.2017.04.022.
[42] R. Roskoski Jr, Vascular endothelial growth factor (VEGF) and VEGF receptor inhibitors in the treatment of renal cell carcinomas, Pharm. Res. 120 (2017) 116–132, https://doi.org/10.1016/j.phrs.2017.03.010.
[43] R. Roskoski Jr, Targeting oncogenic Raf protein-serine/threonine kinases in human cancers, Pharm. Res. 135 (2018) 239–258, https://doi.org/10.1016/j.phrs.2018.08.013.
[44] R. Roskoski Jr, Janus kinase (JAK) inhibitors in the treatment of neoplastic and inflammatory disorders, Pharm. Res. 183 (2022) 106362, https://doi.org/10.1016/j.phrs.2022.106362.
[45] R. Roskoski Jr, Bruton protein-tyrosine kinase (BTK) FDA-approved small molecule inhibitors used for the management of neoplastic and inflammatory disorders, Pharm. Res. 227 (2026) 108187, https://doi.org/10.1016/j.phrs.2026.108187.
[46] M.C. Frame, R. Roskoski Jr, Src family tyrosine kinases. Reference module in life sciences, Elsevier, Amsterdam, 2017, pp. 1–11, https://doi.org/10.1016/B978-0-12-809633-8.07199-5.
[47] R. Roskoski Jr, Targeting BCR-Abl in the treatment of Philadelphia-chromosome positive chronic myelogenous leukemia, Pharm. Res. 178 (2022) 106156, https://doi.org/10.1016/j.phrs.2022.106156.
[48] R. Roskoski Jr, Allosteric MEK1/2 inhibitors including cobimetanib and trametinib in the treatment of cutaneous melanomas, Pharm. Res. 117 (2017) 20–31, https://doi.org/10.1016/j.phrs.2016.12.009.
[49] R. Roskoski Jr, Cyclin-dependent protein kinase inhibitors including palbociclib as anticancer drugs, Pharm. Res. 107 (2016) 249–275, https://doi.org/10.1016/j.phrs.2016.03.012.
[50] R. Roskoski Jr, ERK1/2 MAP kinases: structure, function, and regulation, Pharm. Res 66 (2012) 105–143, https://doi.org/10.1016/j.phrs.2012.04.005.
[51] R. Roskoski Jr, Targeting ERK1/2 protein-serine/threonine kinases in human cancers, Pharm. Res. 142 (2019) 151–168, https://doi.org/10.1016/j.phrs.2019.01.039.
[52] H.S. Meharena, P. Chang, M.M. Keshwani, K. Oruganty, A.K. Nene, N. Kannan, S. S. Taylor, A.P. Kornev, Deciphering the structural basis of eukaryotic protein kinase regulation, PLoS Biol. 11 (2013) e1001680, https://doi.org/10.1371/journal.pbio.1001680.
[53] Y. Liu, K. Shah, F. Yang, L. Witucki, K.M. Shokat, A molecular gate which controls unnatural ATP analogue recognition by the tyrosine kinase v-Src, Bioorg. Med. Chem. 6 (1998) 1219–1226, https://doi.org/10.1016/s0968-0896(98)00099-6.
[54] J.J. Liao, Molecular recognition of protein kinase binding pockets for design of potent and selective kinase inhibitors, J. Med. Chem. 50 (2007) 409–424, https://doi.org/10.1021/jm0608107.
[55] K. Shah, Y. Liu, C. Deirmengian, K.M. Shokat, Engineering unnatural nucleotide specificity for Rous sarcoma virus tyrosine kinase to uniquely label its direct substrates, Proc. Natl. Acad. Sci. 94 (1997) 3565–3570, https://doi.org/10.1073/pnas.94.8.3565.
[56] O.P. van Linden, A.J. Kooistra, R. Leurs, I.J. de Esch, C. de Graaf, KLIFS: a knowledge-based structural database to navigate kinase-ligand interaction space, J. Med. Chem. 57 (2014) 249–277, https://doi.org/10.1021/jm400378w.
[57] G.K. Kanev, C. de Graaf, B.A. Westerman, I.J.P. de Esch, A.J. Kooistra, KLIFS: an overhaul after the first 5 years of supporting kinase research, Nucleic Acids Res. 49 (2021) D562–D569, https://doi.org/10.1093/nar/gkaa895.
[58] V. Modi, R.L. Dunbrack Jr, Kincore: a web resource for structural classification of protein kinases and their inhibitors, Nucleic Acids Res. 50 (2022) D654–D664, https://doi.org/10.1093/nar/gkab920.
[59] R.L. Siegel, T.B. Kratzer, N.S. Wagle, H. Sung, A. Jemal, Cancer statistics, 2026, CA Cancer J. Clin. 76 (2026) e70043, https://doi.org/10.3322/caac.70043.
[60] H. Nguyen, M.S. Habra, Endocrine Malignancies, in: H.M. Kantarjian, R.A. Wolff, A.G. Rieber (Eds.), The MD Anderson Manual of Medical Oncology, fourth ed., McGraw-Hill Education, New York, 2022, pp. 1189–1221.
[61] M. Takahashi, K. Kawai, N. Asai, Roles of the RET Proto-oncogene in cancer and development, JMA J. 3 (2020) 175–181, https://doi.org/10.31662/jmaj.2020-0021.
[62] M. Takahashi, RET receptor signaling: Function in development, metabolic disease, and cancer, Proc. Jpn. Acad. Ser. B Phys. Biol. Sci. 98 (2022) 112–125, https://doi.org/10.2183/pjab.98.008.
[63] M. Takahashi, Four decades of the RET gene: from discovery to tumor-agnostic therapy, J. Formos. Med. Assoc. 124 (2025) 895–901, https://doi.org/10.1016/j.jfma.2025.06.033.
[64] F. Vaio, C. Moliterni, S. Mardente, R. Misasi, E. Mari, State of the art on thyroid cancer biology and oncology, Biomedicines 14 (2026) 168, https://doi.org/10.3390/biomedicines14010168.
[65] Y. Li, P. Wang, J. Cao, H. Liu, Multidisciplinary team diagnosis and treatment of well-differentiated thyroid carcinoma: current landscape and future prospects, Oncologist 31 (2026) oyag017, https://doi.org/10.1093/oncolo/oyag017.
[66] Y. Wei, Y. Zhang, Z. Zhang, Y. Wang, P. Li, Molecular pathogenesis and therapeutic advances in RET fusion-positive papillary thyroid carcinoma, Pathol. Res. Pr. 281 (2026) 156407, https://doi.org/10.1016/j.prp.2026.156407.6.
[67] D.W. Chen, B.H.H. Lang, D.S.A. McLeod, K. Newbold, M.R. Haymart, Thyroid cancer, Lancet 401 (2023) 1531–1544, https://doi.org/10.1016/S0140-6736(23)00020-X.
[68] S.S. Praw, B.J. Gigliotti, A. Tessnow, H. Kang, D.J. Margulies, Executive summary of the 2025 American Thyroid Association management guidelines for adult patients with differentiated thyroid cancer, Thyroid 35 (2025) 1214–1220, https://doi.org/10.1177/10507256251390877.
[69] P. Bellini, F. Dondi, M. Cossandi, G. Viganò, C. Cappelli, E. Gatta, D. Lombardi, R. Morandi, C. Casella, L. Spiazzi, C. Rodella, F. Saiani, C. Ingraito, V. Zilioli, F. Bertagna, The role of ^{123}I in the management of differentiated thyroid cancer: a comprehensive narrative review, Med. Sci. 14 (2026) 68, https://doi.org/10.3390/medsci14010068.
[70] S. Hamidi, M.C. Hofmann, P.C. Iyer, M.E. Cabanillas, M.I. Hu, N.L. Busaidy, R. Dadu, Review article: new treatments for advanced differentiated thyroid cancers and potential mechanisms of drug resistance, Front. Endocrinol. 14 (2023) 1176731, https://doi.org/10.3389/fendo.2023.1176731.
[71] J. Zhang, G. Dionigi, H.Y. Kim, H. Sun, C. Li, Dynamic risk stratification-guided management of medullary thyroid carcinoma: integrating surgical precision with RET-targeted therapies and molecular surveillance, Int. J. Surg. 111 (2025) 7072–7086, https://doi.org/10.1097/JS9.0000000000002816.
[72] C. Romei, R. Ciampi, R. Elisei, A comprehensive overview of the role of the RET proto-oncogene in thyroid carcinoma, Nat. Rev. Endocrinol. 12 (2016) 192–202, https://doi.org/10.1038/nrendo.2016.11.
[73] C. Ricciardi Tenore, E. Tulli, A. Perrucci, R. Bertozzi, L. Fortuna, G. Maneri, C. Santonocito, A. Urbani, M. De Bonis, A. Minucci, *RET* gene alterations in clinical practice: a comprehensive review and database update, Genes 16 (2025) 1472, https://doi.org/10.3390/genes16121472.
[74] Z.J. Zhan, S. Chen, L. Chen, S. Chang, P. Huang, Pediatric thyroid cancer: Distinct pathogenesis, emerging therapeutic strategies and long-term survivorship management, Crit. Rev. Oncol. Hematol. 223 (2026) 105329, https://doi.org/10.1016/j.critrevonc.2026.105329.
[75] G.W. Krampitz, J.A. Norton, RET gene mutations (genotype and phenotype) of multiple endocrine neoplasia type 2 and familial medullary thyroid carcinoma, Cancer 120 (2014) 1920–1931, https://doi.org/10.1002/cncr.28661.
[76] A. Drilon, Z.I. Hu, G.G.Y. Lai, D.S.W. Tan, Targeting RET-driven cancers: lessons from evolving preclinical and clinical landscapes, Nat. Rev. Clin. Oncol. 15 (2018) 150, https://doi.org/10.1038/nrclinonc.2017.188.
[77] J.A. Fagin, S.A. Wells Jr, Biologic and clinical perspectives on thyroid cancer, N. Engl. J. Med. 375 (2016) 1054–1067, https://doi.org/10.1056/NEJMra1501993.
[78] H.J. Hoe, B.J. Solomon, Treatment of non-small cell lung cancer with *RET* rearrangements, Cancer 131 (2025) e35779, https://doi.org/10.1002/cncr.35779.
[79] R. Roskoski Jr, Classification of small molecule protein kinase inhibitors based upon the structures of their drug-enzyme complexes, Pharm. Res. 103 (2016) 26–48, https://doi.org/10.1016/j.phrs.2015.10.021.
[80] P.M. Fischer, Approved and experimental small-molecule oncology kinase inhibitor drugs: a mid-2016 overview, Med. Res. Rev. 37 (2017) 314–367, https://doi.org/10.1002/med.21409.
[81] L. Mologni, C. Gambacorti-Passerini, P. Goekjian, L. Scapozza, RET kinase inhibitors: a review of recent patents (2012-2015), Expert Opin. Ther. Pat. 27 (2017) 91–99, https://doi.org/10.1080/13543776.2017.1238073.

[82] J. Krajewska, T. Gawlik, B. Jarzab, Advances in small molecule therapy for treating metastatic thyroid cancer, Expert Opin. Pharm. 18 (2017) 1049–1060, https://doi.org/10.1080/14656566.2017.1340939.
[83] M. Hochmair, U. Kiiskinen, Y. D'yachkova, T. Puri, X. Wang, S. Wolowacz, A. Vickers, E. Nadal, Matching-adjusted indirect comparison of selpercatinib and pralsetinib in RET fusion-positive non-small cell lung cancer, Future Oncol. 21 (2025) 1867–1878, https://doi.org/10.1080/14796694.2025.2508132.
[84] A. Markham, Selpercatinib: first approval, Drugs 80 (2020) 1119–1124, https://doi.org/10.1007/s40265-020-01343-7.
[85] A. Markham, Pralsetinib: first approval, Drugs 80 (2020) 1865–1870, https://doi.org/10.1007/s40265-020-01427-4.
[86] A.C. Dar, K.M. Shokat, The evolution of protein kinase inhibitors from antagonists to agonists of cellular signaling, Annu. Rev. Biochem. 80 (2011) 769–795, https://doi.org/10.1146/annurev-biochem-090308-173656.
[87] J. Monod, J.P. Changeux, F. Jacob, Allosteric proteins and cellular control systems, J. Mol. Biol. 6 (1963) 306–329, https://doi.org/10.1016/s0022-2836(63)80091-1.
[88] F. Zuccotto, E. Ardini, E. Casale, M. Angiolini, Through the "gatekeeper door": exploiting the active kinase conformation, J. Med. Chem. 53 (2010) 2691–2694, https://doi.org/10.1021/jm901443h.
[89] L.K. Gavrin, E. Saiah, Approaches to discover non-ATP site inhibitors, Med. Chem. Commun. 4 (2013) 41–51, https://doi.org/10.1039/C2MD20180A.
[90] V. Lamba, I. Ghosh, New directions in targeting protein kinases: focusing upon true allosteric and bivalent inhibitors, Curr. Pharm. Des. 18 (2012) 2936–2945, https://doi.org/10.2174/138161212800672813.
[91] J.J. Liao, R.C. Andrews, Targeting protein multiple conformations: a structure-based strategy for kinase drug design, Curr. Top. Med. Chem. 7 (2007) 1394–1407, https://doi.org/10.2174/156802607781696783.
[92] A.J. Kooistra, G.K. Kanev, O.P. van Linden, R. Leurs, I.J. de Esch, C. de Graaf, KLIFS: a structural kinase-ligand interaction database, Nucleic Acids Res. 44 (2016) D365–D371, https://doi.org/10.1093/nar/gkv1082.
[93] B. Wienen-Schmidt, D. Schmidt, H.D. Gerber, A. Heine, H. Gohlke, G. Klebe, Surprising non-additivity of methyl groups in drug-kinase interaction, ACS Chem. Biol. 14 (2019) 2585–2594, https://doi.org/10.1021/acschembio.9b00476.
[94] G.K. Kanev, C. de Graaf, I.J.P. de Esch, R. Leurs, T. Würdinger, B.A. Westerman, A.J. Kooistra, The landscape of atypical and eukaryotic protein kinases, Trends Pharm. Sci. 40 (2019) 818–832, https://doi.org/10.1016/j.tips.2019.09.002.
[95] P. Wu, T.E. Nielsen, M.H. Clausen, FDA-approved small-molecule kinase inhibitors, Trends Pharm. Sci. 36 (2015) 422–439, https://doi.org/10.1016/j.tips.2015.04.005.
[96] V. Subbiah, T. Shen, S.S. Terzyan, X. Liu, X. Hu, K.P. Patel, M. Hu, M. Cabanillas, A. Behrang, F. Meric-Bernstam, P.T.T. Vo, B.H.M. Mooers, J. Wu, Structural basis of acquired resistance to selpercatinib and pralsetinib mediated by non-gatekeeper RET mutations, Ann. Oncol. 32 (2021) 261–268, https://doi.org/10.1016/j.annonc.2020.10.599.
[97] P.P. Knowles, J. Murray-Rust, S. Kjaer, R.P. Scott, S. Hanrahan, M. Santoro, C. F. Ibáñez, N.Q. McDonald, Structure and chemical inhibition of the RET tyrosine kinase domain, J. Biol. Chem. 281 (2006) 33577–33587, https://doi.org/10.1074/jbc.M605604200.
[98] D.M. Vodopivec, M.I. Hu, RET kinase inhibitors for RET-altered thyroid cancers, Ther. Adv. Med. Oncol. 14 (2022) 17588359221101691, https://doi.org/10.1177/17588359221101691.
[99] M. Wei, R. Wang, J. Qian, Q. Fang, J. Tao, Mechanism of and research progress on alterations in the RET gene in thyroid cancer (Review), Mol. Med. Rep. 33 (2026) 164, https://doi.org/10.3892/mmr.2026.13874.
[100] T.S. Gujral, V.K. Singh, Z. Jia, L.M. Mulligan, Molecular mechanisms of RET receptor-mediated oncogenesis in multiple endocrine neoplasia 2B, Cancer Res. 66 (2006) 10741–10749, https://doi.org/10.1158/0008-5472.CAN-06-3329.
[101] B. Salehian, R. Samoa, RET gene abnormalities and thyroid disease: who should be screened and when, J. Clin. Res. Pediatr. Endocrinol. 5 (2013) 70–78, https://doi.org/10.4274/Jcrpe.870.
[102] E. Winer, J. Gralow, L. Diller, B. Karlan, P. Loehrer, L. Pierce, G. Demetri, P. Ganz, B. Kramer, M. Kris, M. Markman, R. Mayer, D. Pfister, D. Raghavan, S. Ramsey, G. Reaman, H. Sandler, R. Sawaya, L. Schuchter, J. Sweetenham, L. Vahdat, R. L. Schilsky, American Society of Clinical Oncology, Clinical cancer advances 2008: major research advances in cancer treatment, prevention, and screening–a report from the American Society of Clinical Oncology, J. Clin. Oncol. 27 (2009) 812–826, https://doi.org/10.1200/JCO.2008.21.2134.
[103] M.J. Niederst, J.A. Engelman, Bypass mechanisms of resistance to receptor tyrosine kinase inhibition in lung cancer, re6, Sci. Signal 6 (2013), https://doi.org/10.1126/scisignal.2004652.
[104] P. Cohen, Protein kinases – the major drug targets of the twenty-first century, Nat. Rev. Drug Discov. 1 (2002) 309–315, https://doi.org/10.1038/nrd773.
[105] P. Cohen, D. Cross, P.A. Jänne, Kinase drug discovery 20 years after imatinib: progress and future directions, Nat. Rev. Drug Discov. 20 (2021) 551–569, https://doi.org/10.1038/s41573-021-00195-4.
[106] M.M. Attwood, D. Fabbro, A.V. Sokolov, S. Knapp, H.B. Schiöth, Trends in kinase drug discovery: targets, indications and inhibitor design, Nat. Rev. Drug Discov. 20 (2021) 839–861, https://doi.org/10.1038/s41573-021-00252-y, https://doi.org/10.1038/s41573-021-00303-4.
[107] A. Mullard, FDA approves 100th small-molecule kinase inhibitor, Nat. Rev. Drug Discov. 24 (2025) 891–895, https://doi.org/10.1038/d41573-025-00188-7.
[108] D.H. Drewry, C.I. Wells, D.M. Andrews, R. Angell, H. Al-Ali, A.D. Axtman, S. J. Capuzzi, J.M. Elkins, P. Ettmayer, M. Frederiksen, O. Gileadi, N. Gray, A. Hooper, S. Knapp, S. Laufer, U. Luecking, M. Michaelides, S. Müller, E. Muratov, R.A. Denny, K.S. Saikatendu, D.K. Treiber, W.J. Zuercher, T. M. Willson, Progress towards a public chemogenomic set for protein kinases and a call for contributions, PLoS One 12 (2017) e0181585, https://doi.org/10.1371/journal.pone.0181585.
[109] N.K. Jha, P. Chauhan, M.M. Abomughaid, D. Avinash, A.G. Almutary, S. Lakhanpal, A. Singh, G.M. Sulaimani, H.M. Al-Kuraishy, H.A. Mohammed, J. Misra, K. Thakur, D. Kumar, mTOR signalling in neurodegenerative disorders: unveiling key factors, mechanistic insights, and possible therapeutic interventions, Cell Physiol. Biochem. 60 (2026) 136–174, https://doi.org/10.33594/000000858.
[110] M. Surma, L. Wei, J. Shi, Rho kinase as a therapeutic target in cardiovascular disease, Future Cardiol. 7 (2011) 657–671, https://doi.org/10.2217/fca.11.51.
[111] Y.Y. Huang, J.M. Wu, T. Su, S.Y. Zhang, X.J. Lin, Fasudil, a Rho-kinase inhibitor, exerts cardioprotective function in animal models of myocardial ischemia/reperfusion injury: a meta-analysis and review of preclinical evidence and possible mechanisms, Front. Pharm. 9 (2018) 1083, https://doi.org/10.3389/fphar.2018.01083.
[112] R. Ahmad, W.H. Frishman, W.S. Aronow, Protein kinase inhibitors in heart failure: mechanistic insights and therapeutic prospects, Cardiol. Rev. (2025), https://doi.org/10.1097/CRD.0000000000001038.
[113] R. Roskoski Jr, Properties of FDA-approved small molecule protein kinase inhibitors: a 2026 update, Pharm. Res. 224 (2026) 108107, https://doi.org/10.1016/j.phrs.2026.108107.
[114] R. Halperin, A. Tirosh, Progress report on multiple endocrine neoplasia type 1, Fam. Cancer 24 (2025) 15, https://doi.org/10.1007/s10689-025-00440-4.
[115] O. Papalou, M. Korbonits, New directions in MEN1 management: navigating the new clinical practice guidelines, Eur. J. Endocrinol. 193 (2025) R71–R82, https://doi.org/10.1093/ejendo/lvaf247.
[116] R. Roskoski Jr, Targeted and cytotoxic inhibitors used in the treatment of breast cancer, Pharm. Res. 210 (2024) 107534, https://doi.org/10.1016/j.phrs.2024.107534.
[117] R. Roskoski Jr, Combination immune checkpoint and targeted protein kinase inhibitors for the treatment of renal cell carcinomas, Pharm. Res. 203 (2024) 107181, https://doi.org/10.1016/j.phrs.2024.107181.
[118] R. Roskoski Jr, Targeted and cytotoxic inhibitors used in the treatment of lung cancers, Pharm. Res. 209 (2024) 107465, https://doi.org/10.1016/j.phrs.2024.107465.
[119] R. Roskoski Jr, Guidelines for preparing color figures for everyone including the colorblind, Pharm. Res. 119 (2017) 240–241, https://doi.org/10.1016/j.phrs.2017.02.005, https://doi.org/10.1016/j.phrs.2018.09.019.